ROLE OF ENDOPLASMIC RETICULUM CALCIUM STORES IN BETA-CELL ER STRESS AND LIPOTOXICITY

by

KAMILA SABINA GWIAZDA

B.Sc., The University of British Columbia, 2006

A THESIS SUBMITTED IN PARTIAL FULFILLMENT OF
THE REQUIREMENTS FOR THE DEGREE OF

MASTER OF SCIENCE

in

THE FACULTY OF GRADUATE STUDIES

(Cell and Developmental Biology)

THE UNIVERSITY OF BRITISH COLUMBIA

(Vancouver)

August 2009

Abstract

There are strong links between obesity, elevated free fatty acids, and type 2 diabetes. Specifically, the saturated fatty acid palmitate has pleiotropic effects on β-cell function and survival. The present study sought to determine the mechanism by which palmitate affects intracellular Ca^{2+} in pancreatic β-cells, and in particular the role of the endoplasmic reticulum (ER). In the MIN6 β-cell line, palmitate rapidly increased cytosolic Ca^{2+} through a combination of Ca^{2+} store release and extracellular Ca^{2+} influx. Palmitate caused a reversible lowering of ER Ca^{2+}, measured directly with the fluorescent protein-based ER Ca^{2+} sensor, D1ER. Using another genetically encoded indicator, long-lasting oscillations of cytosolic Ca^{2+} in palmitate-treated cells were observed. The kinetics of pharmacological SERCA inhibition on the β-cell ER stress response were characterized, and the ER calcium sensor PERK was found to be rapidly activated in response to irreversible ER calcium depletion. ER calcium depletion in palmitate-treated cells also induced rapid phosphorylation of PERK, as well as other subsequent downstream ER stress signals. In summary, the effects of the free fatty acid palmitate on pancreatic β-cell Ca^{2+} homeostasis were characterized in this thesis. This study provides the first direct evidence that free fatty acids reduce ER Ca^{2+} and sheds light on pathways involved in β-cell ER stress, lipotoxicity and the pathogenesis of type 2 diabetes.

Table of Contents

List of Tables

List of Figures

List of Abbreviations

AUC	Area under the curve
ATF6	Activating transcription factor 6
BSA	Bovine serum albumin
Ca^{2+}	Calcium
CHOP	C/EBP-homologous protein
eIF2α	Eukaryotic translation initiation factor 2 alpha
ER	Endoplasmic reticulum
FBS	Fetal bovine serum
FFA	Free fatty acid
FRET	Fluorescence resonance energy transfer
GPR40	G-protein coupled receptor 40
IP_3R	Inositol 1,4,5-triphosphate receptor
IRE1	Inositol requiring ER-to nucleus signal kinase 1
LC-CoA	Long-chain acyl-coenzyme A
RyR	Ryanodine receptor
MIN6	Mouse insulinoma
PBS	Phosphate-buffered saline
PERK	Double-stranded RNA-activated protein kinase-like ER kinase
UPR	Unfolded protein response
XBP-1	X-box binding protein-1

Acknowledgements

The past two years have been a roller-coaster ride, and I am very grateful to everyone who helped me to get to where I am. First and foremost, my supervisor, Jim Johnson, who has inspired and motivated me, and has shaped the scientist I have become. His sheer love of science is contagious, and I will miss his uncanny way to make everything funny. Jim, thanks for putting up with my anxiety and seemingly never-ending capacity for stress; it's not easy to do. Thank you for showing me that I can actually do this. My committee members, Chris Loewen, Tim Kieffer, and Eric Jan: thank you for all your guidance, your suggestions and your support.

To everyone in the lab, past and present, who has inspired and helped me: Emilyn, Dan, Tatyana, Yalin, Ting, Jessica, Carol, Arya, Connie, Farnaz, Betty, Grace, Erin. Em, you were always there for me, and we've had a lot of fun, both in the lab and out. I'll never forget our trip to Ireland, dancing and singing in the lab, and everything in between. Dan, thanks for teaching me pretty much everything I know (about everything!) and for all your advice. And to everyone else, thanks for all your kindness and help, and most of all thanks for putting up with me in the lab and for providing such a great work environment. I'll miss you all!

And most importantly, to my family: my sister, dad, and mom. Thank you for supporting me and being there for me through the years. Special thanks to my sister, for keeping me sane and laughing, and my dad for inspiring me and pushing me to work hard.

It's not over 'til it's over, so you may as well enjoy the ride.

KG

Chapter One: Introduction

Type 2 diabetes has become a disease of epidemic proportions, and is no longer limited to Western countries and cultures. The World Health Organization (WHO) estimates that the disease now affects over 180 million people, causing approximately 2.9 million deaths each year (124). Associated complications of diabetes include retinopathy, neuropathy, limb amputations, kidney failure, and increased risk for heart disease and stroke, rendering type 2 diabetes an important medical concern and a severe health care burden. The numbers of diabetes cases are expected to double between 2000 and 2030 (156), and consequently the WHO estimates that over the next 10 years diabetes deaths will increase by more than 50% without urgent action (155). There is no current cure for diabetes, only treatment to manage it and at best slow its progression. Together, these statistics indicate that this epidemic is only going to increase and continue affecting people the world over.

Pathophysiology of Type 2 Diabetes

Type 2 diabetes is caused by peripheral insulin resistance, insulin secretory defects, and programmed cell death of the pancreatic insulin-secreting β-cells (16, 35, 126, 161). The best-known risk factor for the disease is obesity, which is characterized by elevated levels of circulating plasma free fatty acids (12). The lipid levels are elevated due to expanded and highly lipolytic stores of adipose tissue (12, 116). Obesity itself is associated with insulin resistance in tissues such as muscle, liver, and adipose, but most obese and insulin-resistant individuals do not develop type 2 diabetes because their β-cells can compensate by increasing their β-cell mass and hyper-secreting insulin (67). The disease occurs when

peripheral insulin resistance is too great and β-cells can no longer secrete the required amounts of insulin, or when the β-cells themselves fail and undergo apoptosis (16, 115). There are many causes of β-cell dysfunction and apoptosis in type 2 diabetes: hyperglycemia, hyperlipidemia, pro-inflammatory cytokines, and secreted islet amyloid polypeptide. Whether these factors are causal or secondary to the disease state, or both, is difficult to determine, but it is clear that to further understand diabetes pathophysiology, the biology of the pancreatic islet β-cell must be better understood.

Obesity and lipotoxicity

The link between obesity and diabetes is robust. The vast majority (>80%) of patients with type 2 diabetes are obese and most obese individuals have symptoms of pre-diabetes, including impaired glucose tolerance and insulin resistance. Lipotoxicity, the phenomenon whereby excess fatty acids cause cell death, helps explain how elevated levels of lipids, such as those seen in obesity, can be detrimental to pancreatic β-cell health. Insulin resistance, considered to be one of the first steps in the onset of type 2 diabetes, also results from toxic amounts of saturated fatty acids in insulin-sensitive tissues, including the liver, adipose and muscle (91, 158). In some *in vivo* models of obesity, such as the Zucker diabetic fatty (ZDF) rat that develops obesity and diabetes, β-cell apoptosis is seen in the obese pre-diabetic state, when the islets are fat-laden (132). Indeed, many *in vitro* experiments using human and rodent primary islets as well as cultured β-cells have shown that chronic elevation of the long-chain saturated fatty acid palmitate induces β-cell death (68, 83, 85, 110, 132). In contrast, *in vitro* studies using treatments with monounsaturated fatty acids such as palmitoleate (C16:1) and oleate (C18:1) found that these lipids tend to be

less cytotoxic (26, 49, 68, 70, 90), and in some cases even protective, against palmitate toxicity (32, 85, 86).

Some investigators suggest that the toxic effects of lipids occur only concurrently with high levels of glucose, a phenomenon termed glucolipotoxicity (111-113). A recent report suggested that elevated glucose levels accentuate lipotoxicity *in vitro*, through the regulation of ER stress by the protein synthesis activator mTORC1 (7). However, it is conceivable that hyperlipidemia may affect β-cell survival and function in the absence of hyperglycemia and frank diabetes, suggesting that lipids can indeed have deleterious effects on β-cells on their own, as has been shown *in vitro* (26, 85, 86, 125, 162). Further, *in vitro* studies using obese pre-diabetic ZDF rats demonstrate lipotoxicity and β-cell dysfunction in the absence of elevated glucose levels (50). To add further complexity to this issue, high glucose itself can induce lipotoxicty by up-regulating lipogenic genes (150), thereby creating a cellular glucolipotoxic environment separate from that caused by elevated plasma lipid levels alone. Whether the two stimuli act additively or synergistically once diabetes has been established remains to be determined.

Measuring plasma free fatty acid levels

Fatty acids are essential nutrients and physiological signalling molecules, and as such there exists a spectrum of plasma free fatty acid levels that range from normolipidemic to hyperlipidemic. Under normal conditions, the vast majority of circulating plasma fatty acids are bound to carrier proteins. The most abundant of these carrier proteins is albumin, which also has the highest affinity for free fatty acids (134). However, in states where the fatty acid to albumin ratio is high (> 4:1) other molecules such as lipoproteins and phospholipid vesicles can also bind fatty acids (21). In healthy individuals, the molar ratio of

fatty acids to albumin ranges from 0.5:1 to 2:1 (24), while in conditions including obesity and diabetes, the ratio can increase up to 6:1 (117). There are at least 43 different FFA species present in human plasma, but in FFA preparations from human plasma albumin, the C16 and C18 FFA's accounted for 90% of total FFA (17). Additionally, palmitate is the predominant lipid produced by *de novo* lipogenesis (1), and this pathway contributes 20% of the palmitate stored in adipose tissue (138).

Determining the concentration of free fatty acid circulating in plasma is complicated by the FFA: albumin ratio, as the binding of one fatty acid affects the binding of subsequent fatty acids to albumin (134). The presence of lipases (hormone-sensitive lipase and adipocyte triglyceride lipase) in the β-cell also increases endogenous FFA levels (40, 109). Nevertheless, the total level of palmitate in plasma of healthy humans in one study ranged from 720 μM to 2 mM (17), and a suggested healthy range of unbound FFA is 7.5 ± 2.5 nM (121). By comparison, a solution containing 0.5 mM palmitate in a 5:1 FFA: BSA ratio, a typical amount used in *in vitro* studies, gave a free palmitate concentration of 200 nM (112). It should also be noted that the levels of bound free fatty acids in the obese and diabetic ZDF rat were greater than 1 mM (132). Together, these studies demonstrate that there is quite a range of plasma free fatty acid levels, and re-creating a physiological fatty acid milieu *in vitro* can be difficult.

Fatty acids and insulin secretion

Acute administration of fatty acids, especially palmitate, is thought to cause a modest increase in insulin secretion (25, 98), while prolonged exposure to this fatty acid increases basal insulin secretion and decreases the relative response to glucose both *in vitro* and *in vivo* (9, 13, 102, 163). Additionally, circulating fatty acids are thought to be critical in

maintaining glucose-stimulated insulin secretion after fasting (33, 34). However, the mechanisms by which palmitate affects β-cell insulin secretion are not fully understood. There has been recent evidence pointing to the involvement of the long-chain fatty acid G-protein coupled receptor GPR40 (60, 69, 76, 96, 136, 141), though the effects of acute vs. chronic palmitate treatment on GPR40 activation remain controversial (3). Additionally, fatty acid uptake via CD36 and consequent intracellular signalling is also involved (99), and the literature suggests mechanisms involving altered mitochondrial metabolism (13), signalling through esterified long-chain CoA molecules (107, 114, 123), and insulin granule exocytosis (101). Intracellular lipolysis and FFA/triglyceride cycling may also play a role in insulin secretion (40, 109). Indeed in the Zucker fatty rat, which is obese but does not develop diabetes, lipolysis has been suggested as the mechanism by which the β-cells compensate for insulin resistance by enhancing insulin secretion (97).

Mechanisms of lipotoxicty

There are many proposed models that account for toxic effects of chronically elevated lipids (146). One model of lipotoxicty hypothesizes that free fatty acids, especially palmitate, cause ER stress, the state in which the endoplasmic reticulum of a cell cannot cope with its protein load and initiates the unfolded protein response (UPR). If the ER stress signals are chronically elevated, they can eventually lead to apoptosis (128). Lipotoxicity has also been examined in the context of oxidative stress, ceramide generation, and altered lipid partitioning, but these models are not mutually exclusive from the ER stress model.

ER stress in the β-cell

Pancreatic β-cells are especially susceptible to the unfolded protein response (UPR) and endoplasmic reticulum (ER) stress, as they are high capacity secretory cells with a extensive network of ER. The ER stress response is activated under pathological conditions, but also as a normal physiological response to secure ER integrity. The UPR has three main functions. One function is to up-regulate ER chaperone proteins to help reduce the load of misfolded proteins. A second function is to decrease the overall rate of protein synthesis, while sparing proteins that are required for the UPR. A third function involves the initiation of programmed cell death, once the cell decides that it can no longer be saved (54). The ER trans-membrane proteins IRE1, PERK, and ATF6 initiate these signals by sensing an increase in the misfolding of ER client proteins. Once activated, these proteins activate their respective targets (**Fig. 1**). IRE1, an endonuclease and kinase, cleaves cytosolic XBP-1 mRNA, activating the transcription factor to transcribe ER stress-inducible genes, such as chaperones, to aid in protein folding. Chronic IRE1 signalling has also been shown to activate JNK and initiate apoptosis (147). PERK phosphorylates eIF2α, causing a general attenuation of translation in order to decrease the protein load on the ER. ATF6 is a transcription factor that also up-regulates ER stress-inducible target genes. Together, these molecules are the proximal UPR signals, and if chronically activated, can initiate programmed cell death through pro-apoptotic molecules such as CHOP and JNK.

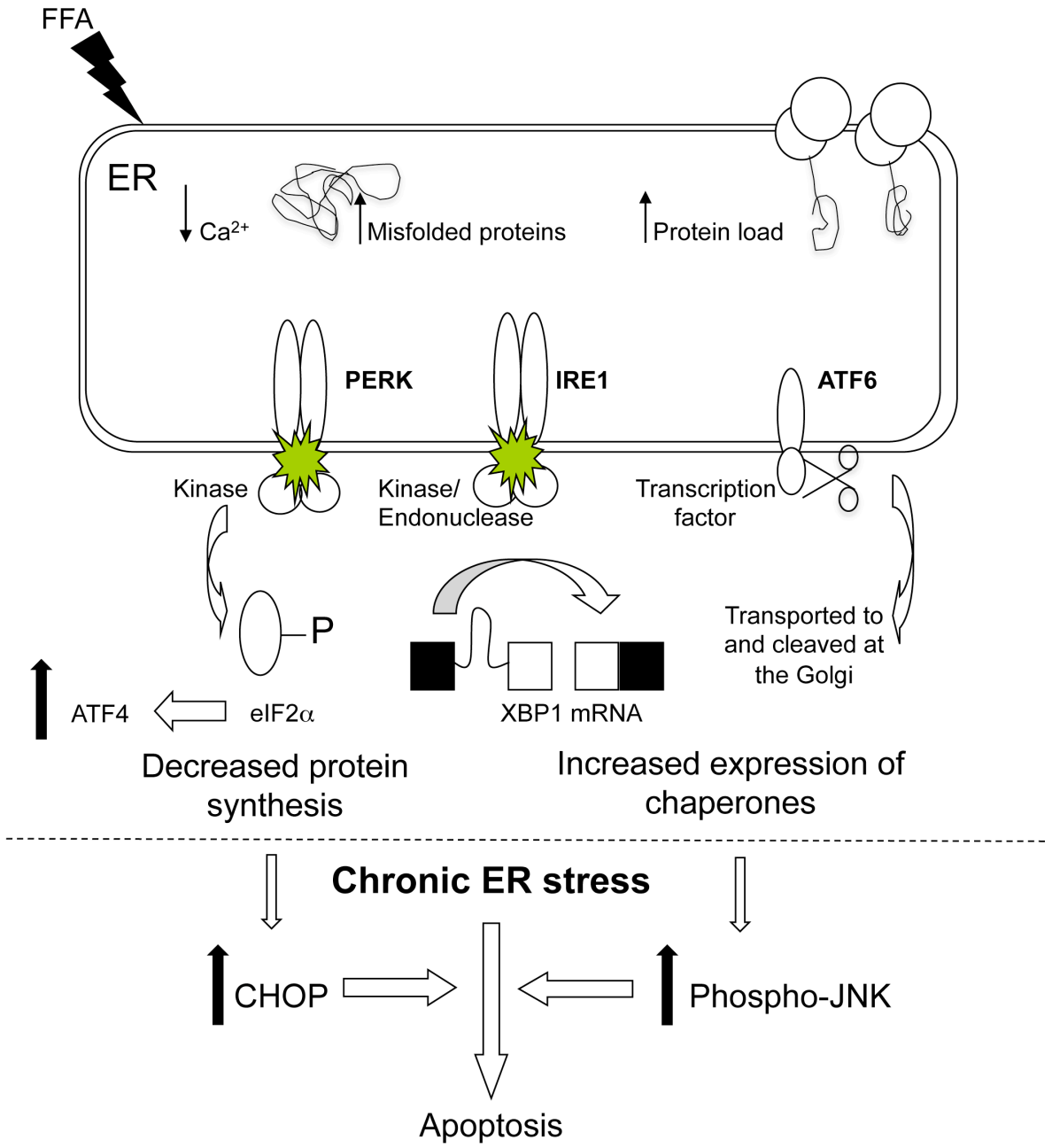

Figure 1. Schematic of the ER stress signalling cascade in the beta-cell. Thick arrows indicate an increase in protein levels. The diagram is not to scale and many molecules have been left out for simplicity.

ER stress and diabetes

There are a number of mutations that disrupt the protein folding pathway that lead to diabetes, including those found in permanent neonatal diabetes, Wolfram syndrome, and

Wolcot-Rallison syndrome (128). In the Akita mouse, the Insulin 2 gene carries a mutation similar to those found a subset of patients with neonatal diabetes (137), which prevents the formation of an essential disulphide bond and causes the protein to misfold and become retained in the ER. Over time, the Akita mouse develops diabetes due to a progressive loss of its β-cell mass, a consequence of excessive ER stress-induced apoptosis (103). A loss of PERK also causes a loss in β-cell mass and diabetes in mice (55), and in humans this mutation is known as the autosomal recessive Wolcot-Rallision syndrome, which also results in diabetes (30). Wolfram syndrome, a human autosomal recessive neurodegenerative disorder that also presents with juvenile-onset diabetes (8), is caused by a mutation in *WFS1*, an ER resident protein that is likely involved in ER protein degradation (54). Additionally, polymorphisms in the transcription factor ATF6 have been associated with type 2 diabetes in two different population studies (94, 143). Other mouse models have been made to further elucidate the effects of ER stress signalling machinery, including the $eIF2\alpha^{Ser51A}$ mouse, which develops diabetes due to PERK's inability to phosphorylate the mutated eIF2α (133). A number of studies also demonstrate the role of islet-amyloid polypeptide toxicity, and suggest that the excess presence of this toxic protein contributes to β-cell failure through ER stress (58, 92). Together, these conditions underline the importance of ER homeostasis in β-cells and the requirement of intact ER stress machinery for healthy β-cell function and normal glucose homeostasis (128).

Lipotoxicty and ER stress

Many studies have found that fatty acids, specifically palmitate, initiate β-cell ER stress *in vitro* (26, 39, 68, 77), as well as *in vivo* (77). Studies with fatty acids oleate and palmitoleate have found these monounsaturated fats to induce less ER stress than palmitate

in some models (26, 70, 90), and none at all in others (31, 32, 68). How fatty acids induce ER stress remains unclear, but recent reports point to a few different mechanisms. For example, chronic treatment with palmitate, but not oleate, caused morphological distention of the ER, which could affect its function and induce the stress response (68). Saturated fats, owing to their high melting point, are more likely to precipitate once formed, while unsaturated fats can be safely stored as triglycerides. Saturated fats also affect membrane fluidity, causing an increase in rigidity and hampering membrane function (139). Palmitate has also been shown to feed into *de novo* ceramide synthesis (108), which can activate apoptosis in ZDF rat islets (132). A recent study also found that palmitate directly affected the degradation of an important insulin-processing enzyme, carboxypeptidase E (CPE) (62). Further, β-cells exhibited significant ER stress and apoptosis in mice lacking CPE, indicating that this enzyme is required for β-cell survival and function (62).

A recently discovered effect of palmitate is its ability to elicit intracellular calcium (Ca^{2+}) signals in rodent islets and some β-cell lines (118, 129). The ER is a major cellular Ca^{2+} store and ER Ca^{2+} homeostasis is critical for ER function (130), and importantly, insulin processing (52). Accordingly, depletion of ER Ca^{2+} by cytokines or inhibitors of the ER Ca^{2+} uptake pump (SERCA) can trigger an extensive ER stress response in β-cells (18, 81). A recent report documented that blocking Ca^{2+} entry through voltage-gated Ca^{2+} channels inhibited palmitate-induced β-cell apoptosis (62). This may provide a potential link between palmitate, ER stress, and lipotoxicity.

Lipotoxicity and Ca^{2+} signalling

Whether palmitate directly affects ER Ca^{2+} stores remains unclear. Recent studies employing indirect measurements of the ER filling state in INS-1 cells (68) and mouse islets

(101) failed to detect any effects of palmitate on ER Ca^{2+} homeostasis. In other studies, palmitate was shown to increase cytosolic Ca^{2+} levels in HIT-T15 and INS-1 cells, as well as primary mouse β-cells (118, 129). In HIT-T15 cells, the maintenance of these signals was dependent on extracellular Ca^{2+} influx through voltage-gated Ca^{2+} channels (118). However, the observation that a Ca^{2+} transient remained in the absence of extracellular Ca^{2+} suggested that a component of these Ca^{2+} signals might be initiated by intracellular stores (118). It is thought that the G-protein coupled receptor for long-chain fatty acids, GPR40 (15, 60, 73), may play a role in initiating palmitate-induced Ca^{2+} signals. Activation of G-protein coupled fatty acid receptors would be expected to mobilize IP_3-sensitive Ca^{2+} stores on the ER (15, 60, 73). Notwithstanding, the effects of palmitate on ER Ca^{2+} levels have not been measured directly using targeted ER Ca^{2+} sensors (106). Although these previous studies suggest that Ca^{2+} dynamics play an important role in the effects of palmitate, the precise mechanisms by which palmitate affects β-cell Ca^{2+} homeostasis remain unresolved.

Ca^{2+} signalling in the β-cell

Ca^{2+} is a ubiquitous second messenger in cells, involved in a vast array of cellular processes including growth, gene regulation, proliferation, metabolism, exocytosis, and apoptosis (10, 22, 122). Persistently elevated Ca^{2+} is toxic to cells, and thus its levels must be carefully regulated. Cytosolic baseline levels of Ca^{2+} are typically in the 100 nM range, about 20,000 times lower than the extracellular environment (22). The ER serves as a major intracellular Ca^{2+} store, storing micromolar amounts of the molecule (105). Ca^{2+} signals themselves, whether initiated extrinsically or intrinsically, are coded in a variety of ways: transient rises in Ca^{2+} can vary in amplitude, frequency, and spatial localization; they can rise locally at a mouth of a channel, be confined to one area of a cell, or propagate in a

global wave that can then spread between cells (122). These Ca^{2+} signals can originate from channels on the ER, the IP_3R- and RyR-gated channels, from the various channels and pumps on the plasma membrane, or from other organelles such as the Golgi apparatus and mitochondria. Additionally, there are many channels and pumps that buffer Ca^{2+}, to turn signals off and return the cytosol to baseline levels, including the ER Ca^{2+} uptake pump, SERCA. Together, these mechanisms serve as the cellular Ca^{2+} signalling toolkit (11), creating a complex code of signals that can control a vast array of cellular processes.

Well-studied examples of Ca^{2+} signalling occur in secretory cells, such as the pancreatic β-cells. The combination of cellular Ca^{2+} channels and pumps creates cytosolic Ca^{2+} oscillations that drive oscillatory insulin secretion in glucose-stimulated β-cells (142). The cascade of events leading to glucose-stimulated Ca^{2+} signals in β-cells starts when glucose is internalized by the transporter GLUT2 (or GLUT1 in humans) (27), undergoes glycolysis and oxidative metabolism, and increases the cell ATP/ADP ratio. ATP inhibits plasma-membrane K_{ATP} channel activity, resulting in cell depolarization and activation of voltage-dependant Ca^{2+} channels on the plasma membrane (5). The local increase in sub-plasma membrane Ca^{2+} regulates docking and fusion of secretory granules, resulting in insulin secretion (84, 157). Importantly, this secretion is pulsatile in nature, and consequently creates oscillations in plasma insulin levels, which are important for insulin action on its target tissues. This pulsatility is controlled by oscillations in cytosolic Ca^{2+}, among other factors, and this in turn is triggered by the oscillatory nature of glucose metabolism (57). These oscillations in Ca^{2+} are dependent on both voltage-gated extracellular Ca^{2+} influx as well as the sequestration of cytosolic Ca^{2+} into the ER via SERCA pumps (142). There are different types of oscillations: slow, fast, spiking, and fast

receptor-induced, and they are controlled by different stimuli (glucose, IP_3, cAMP) and result in different frequencies and durations of intracellular Ca^{2+} increase (142). However, all of the intricate mechanisms in insulin secretion have not been fully elucidated. Other aspects of cellular metabolism, including pyruvate cycling, NADH, cAMP, and PLC-mediated agonists, may also play a part in glucose-stimulated insulin secretion (57, 63, 82, 142).

Imaging intracellular Ca^{2+}

To measure the intricacies of intracellular Ca^{2+} signals, probes have been developed that allow real-time live-cell imaging of intracellular Ca^{2+} dynamics. These probes, which have varying degrees of sensitivity, stability, and versatility, are molecules whose light absorption or emission properties change upon calcium binding, through a change in intensity or spectral shift. Since the development of the first fluorescent Ca^{2+} indicators (51), a variety of probes have been developed that are either small molecule fluorescent indicators (i.e. dyes), aequorin-based chemiluminescent Ca^{2+} sensors, or genetically encoded Ca^{2+} indicators (104).

The most widely used small molecule Ca^{2+} indicators include Fura-2, Fluo-3 and Fluo-4, and they differ with respect to their resistance to photobleaching, compartmentalization, leakage, loading, and dynamic range (144). These molecules are used to measure cytosolic Ca^{2+} levels and have proved very useful for measuring transient rises and oscillations. The next class of indicators, which is based on the jellyfish aequorin photoprotein, generates light upon calcium binding to the aequorin in the presence its prosthetic group, coelenterazine. Among the advantages of using aequorin-based indicators is that there is a very high signal to noise ratio, given that no mammalian cell produces any

luminescent molecules. Importantly, aequorins can be targeted to organelles and engineered to have the correct dynamic range for the organelle (4). In contrast to dyes like Fura, they have low calcium buffering capacity, preventing them from significantly affecting intracellular Ca^{2+} homeostasis. However, single-cell imaging is difficult with aequorins because only one photon is released per probe, giving a low level of light emission per cell, in contrast to the strongly emitting fluorescent dyes. More importantly, the reconstitution of aequorin with its cofactor is difficult, requiring the compartment to have low Ca^{2+} levels. For imaging Ca^{2+} within organelles such as the ER where Ca^{2+} levels are high, this step requires lowering ER Ca^{2+}, using ionophores and inhibitors of the SERCA uptake pumps, which causes a significant alteration of organelle physiology (14).

The last class of probes is the fluorescent protein-based genetically encoded indicators. These molecules have been designed with a calcium-responsive element, such as calmodulin, present with either one or two fluorescent proteins. In the single-fluorescent protein probes, termed camgaroos and pericams, the binding of Ca^{2+} alters the structure of the molecule, causing a change in its spectral properties. Probes containing two fluorescent proteins, the cameleons, are engineered such that Ca^{2+} binding changes the degree of fluorescence resonance energy transfer (FRET) between two fluorophores (93). Like aequorins, because these probes are based on recombinant cDNA expression, they can be targeted to various cellular compartments and organelles using targeting sequences. Alternatively, transgenic lines or animals can be made that express these constructs (6, 41). In contrast to the aequorins, however, these probes are easy to work with, provided they can be transfected into the cells of interest. By comparison, the fluorescent dyes tend to have faster reaction kinetics, better dynamic range, and increased sensitivity than the current

genetically encoded calcium indicators. However, because cells loaded with these dyes suffer from problems like dye leakage, compartmentalization, and photobleaching, the genetically engineered sensors are uniquely suitable for long-term Ca^{2+} imaging experiments. This is important given that the long-term dynamics of cellular Ca^{2+} have not been measured in most cell types, including pancreatic β-cells.

Some recently developed cameleons have been fine-tuned to perform well in specific compartments, including the ER and the cytoplasm. These 'newer generation' cameleons are less affected by fluctuating pH levels and have improved dynamic range over their predecessor cameleons (106). Additionally, they are not affected by nor do they affect endogenous calmodulin levels, which was a problem with earlier versions of the probes (93). Two of these probes, D3cpv and D1ER, are specifically targeted to the cellular cytoplasm (D3cpv) and ER (D1ER) (**Fig. 2**). Both have appropriate dynamic ranges for their compartments: the affinity of D3cpv for Ca^{2+} is much higher than D1ER, reflecting the lower Ca^{2+} levels in the cytoplasm (93). D1ER is efficiently targeted to its organelle by virtue of an ER signal sequence as well as an ER retention sequence (81), and D3cpv is limited to the cytoplasm by its lack of signalling sequence. Thus, the D1ER probe presents the best method for dynamically imaging physiologically relevant luminal Ca^{2+} changes within β-cells (62, 105), and D3cpv allows for accurately imaging cytosolic Ca^{2+} signals for extended periods of time.

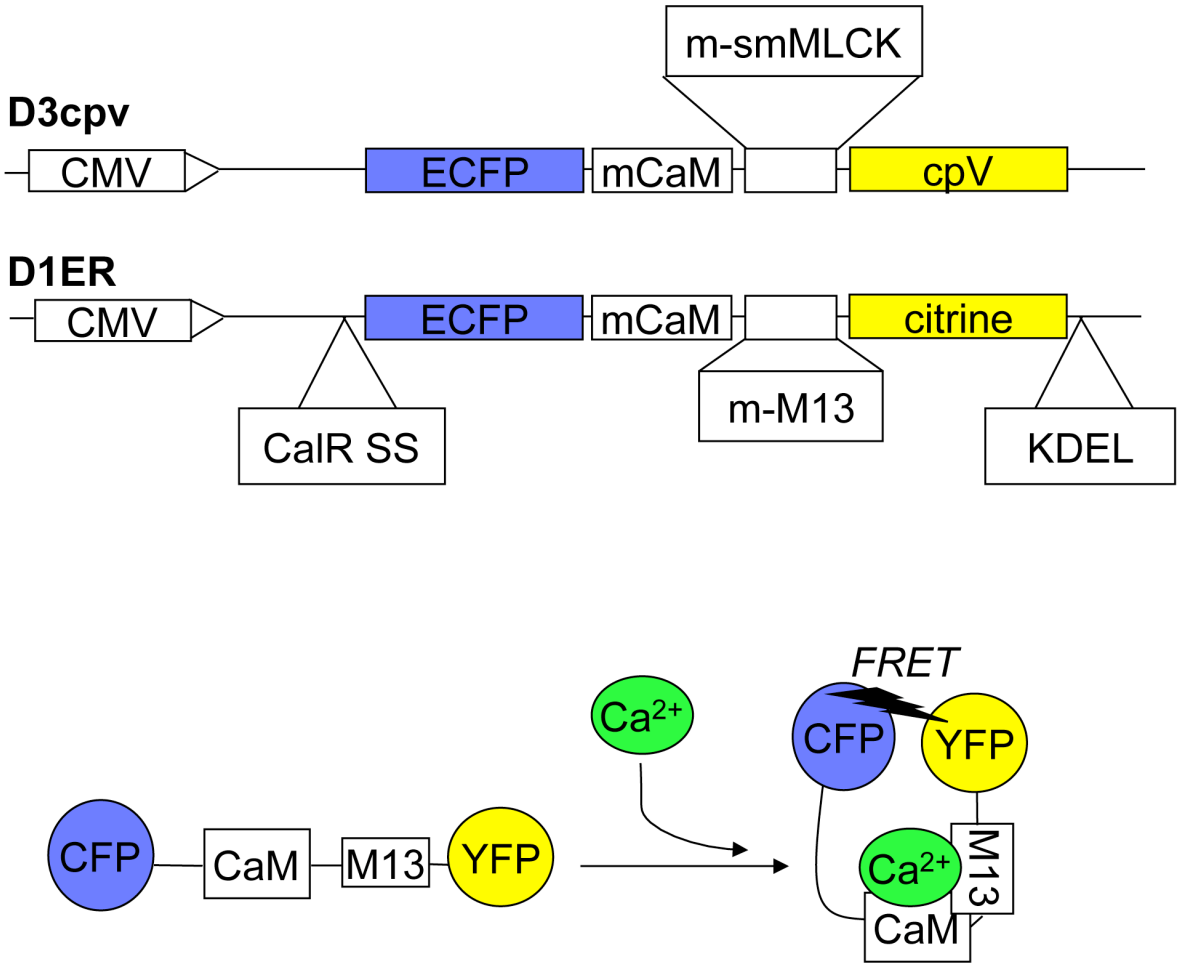

Figure 2. . Schematic of the genetically engineered cameleon constructs and Ca^{2+}-stimulated FRET. (**A**) Schematic of the genetically encoded cameleons D3cpv (cytosol) and D1ER (ER). 'm' indicates mutant; CaM, calmodulin; smMLCK, smooth muscle myosin light chain kinase; cvV, circularly permuated Venus; CalR SS, calreticulin signal sequence; M13, peptide from skeletal muscle myosin light chain kinase; KDEL, ER retention tag sequence. (**B**) Schematic representation of Ca^{2+}-stimulated FRET between the generic CFP/YFP cameleon. The diagram is not to scale.

Caspases and apoptosis in β-cells

Caspases are a family of cysteine-requiring aspartate proteases that are key in regulating the initiation and execution of apoptosis in β-cells (59). To denote their function in the apoptotic pathway, they are classified as initiator (early activation) or effector (late mediator) caspases. Caspase 9, an initiator caspase, is activated by cytochrome c, released

from compromised mitochondria, together with Apaf-1 in the presence of dATP (59). Caspase 9 then activates pro-caspase 3, an effector executioner caspase, pro-caspase 7 and other apoptosis factors including PARP, to induce the hallmarks of apoptosis: cell blebbing, chromatin condensation, protein cross-linking, and collapse of nuclear membrane (59). In rodents, caspase 12, which is located at the ER membrane, is activated in response to ER stress by IRE1 and cleaved by Caspase 7 or *m*-Calpain (54) and leads to caspase 3 activation. However, caspase-12 is thought to be a pseudogene in man, and therefore may not have an evolutionarily conserved role (42), although whether or not it is important in human ER stress signalling remains controversial (88, 140, 159). Indeed, altering ER Ca^{2+} homeostasis by drugs that block ER Ca^{2+} uptake caused ER stress-induced caspase 3 activation in β-cells (81). Thus these proteins are potent executors of apoptotic cell death, but the field of caspase biology is limited in its knowledge of caspase activation kinetics.

Chapter Two: Materials and Methods

Reagents

All reagents were from Sigma (St. Louis, MO), unless otherwise indicated. The acetoxymethyl ester of the cytoplasmic Ca^{2+} dye Fura-2 (Fura-2-AM; Molecular Probes; Eugene, OR) was stored in dimethyl sulfoxide (DMSO) as a 1 mM stock solution. Thapsigargin, xestospongin C (Cayman Chemical; Ann Arbor, MI), and nifedipine (Calbiochem; San Diego, CA) were stored in DMSO as a 1 mM stock solution, and ryanodine (Tocris Biosciences; Ellisville, MO) was stored in DMSO as a 100 mM stock solution. Carbachol (Calbiochem; San Diego, CA) was dissolved in water to a 100 mM stock solution. The cameleon FRET probes D1ER and D3cpv were gifts from Dr. Amy Palmer (Department of Chemistry and Biochemistry, University of Colorado). Drug solutions were prepared immediately before each experiment.

Palmitic acid (Nu-Check Prep; Elysian, MN) was dissolved in 65 mM NaOH and complexed with 20% essentially fatty-acid free bovine serum albumin (BSA). The complex was added to Dulbecco's Modified Eagle Medium (DMEM, Invitrogen; Burlington, ON) containing 5 mM or 25 mM glucose, 10% fetal bovine serum (Invitrogen; Burlington, ON) and 1% penicillin-streptomycin (Invitrogen; Burlington, ON) for a final molar ratio of 6:1 palmitate to BSA (21), unless otherwise indicated. For imaging experiments, sodium palmitate was prepared as described (118). Briefly, a stock solution of 100 mM was prepared by dissolving palmitate in 60 mM NaOH and added to pre-warmed Ringer's solution (3 mM glucose) containing 0.1% essentially fatty acid free BSA in a 6:1 molar ratio. 2-bromopalmitate solutions were prepared in the same way. Oleate solutions were

prepared as described (129), by dissolving oleic acid in hot (95°C) 100 mM NaOH to a 100 mM stock solution, and diluted by addition to pre-warmed Ringer's solution containing 0.1% essentially fatty acid free BSA in a 6:1 molar ratio. For imaging experiments, the final concentration of palmitate, oleate, and 2-bromopalmtiate was 100 μM unless otherwise shown. Vehicle controls contained BSA and NaOH, and did not induce cell death or Ca^{2+} fluxes (data not shown).

Table 1. List of antibodies used

Antibody (Ab)	1° Ab dilution	Incubation	2° Ab source, dilution	Company
Phospho-PERK	1:500, 5% BSA	48 hours	Rabbit, 1:1000	Cell Signalling
Phospho-eIF2α	1:500, 5% BSA	48 hours	Rabbit, 1:1000	Cell Signalling
eIF2α	1:1000, I-Block	24 hours	Mouse, 1:2500	Abcam
XBP-1	1:200, I-Block	24 hours	Rabbit, 1:2000	Santa Cruz
CHOP	1:200, I-Block	24 hours	Rabbit, 1:1000	Santa Cruz
Cleaved caspase 3	1:1000, I-Block	24 hours	Rabbit, 1:1000	Cell Signalling
Cleaved caspase 9	1:1000, I-Block	24 hours	Rabbit, 1:1000	Cell Signalling
Cleaved caspase 12	1:1000, I-Block	24 hours	Rabbit, 1:1000	Cell Signalling
β-actin	1:30,000, I-Block	24 hours	Mouse, 1:10,000	Novus

MIN6 Cell Culture

The mouse insulinoma-derived (MIN6) cell line (95) was cultured as described (36). MIN6 cells were grown to a confluence of 30%-60% for cameleon or fura-2 imaging, and to a confluence of 80-90% for cell treatment and protein extraction. For cameleon imaging, MIN6 cells were transfected with D1ER or D3cpv cameleon DNA one day after seeding on sterile 22 mm coverslips using 1μg Lipofectamine 2000 reagent (Invitrogen, Burlington, ON) per coverslip and 1 μg/uL midi-prepped construct DNA in 50 μL Opti-MEM (Invitrogen, Burlington, ON). Cells were left to take up DNA for 4-6 hours, then fresh

DMEM was added and cells were imaged within 2-3 days.

Live-cell Imaging

Single-cell imaging was performed in HEPES-buffered Ringer's solution containing 144 mM NaCl, 5.5 mM KCl, 1 mM $MgCl_2$, 2 mM $CaCl_2$, 20 mM HEPES, and 3 mM glucose, unless otherwise indicated (64). Cytosolic Ca^{2+} was imaged in Fura-2-AM-loaded cells as described previously (64, 80), or in D3cpv-expressing cells (106). ER luminal Ca^{2+} was imaged using the FRET-based D1ER cameleon (105, 106). Pre-heated solutions were applied by stable perifusion at 1 ml/minute and complete solution changes were achieved in <30 seconds. Images were taken using a 10x objective, unless otherwise indicated, with a Zeiss 200m inverted microscope, a Sutter Lambda DG4 excitation source, a Roper CoolSnap HQ2 camera and Slidebook Software (Intelligent Imaging Innovations, Denver, CO). The CFP component of the cameleons was excited at 430 nm using a S430/25x filter (Chroma). CFP emission and YFP (FRET) emission were alternately collected at 470 and 535 nm respectively, using S470/30m and S535/30m filters mounted in a Sutter Lambda 10-2 emission filter wheel. The FRET signal was normalized to the CFP emission intensity, and changes in ER or cytosolic Ca^{2+} were expressed as the FRET/CFP ratio. There was no correlation between the apparent Ca^{2+} levels and the intensity of the FRET probes (D3cpv and D1ER) in the cells used for this study (data not shown). The analysis of D1ER-measured ER Ca^{2+} responses was performed on a cell-by-cell basis. A response was considered to have occurred if: 1) there was an inflection of the calcium signal within the treatment period that deviated from baseline by >15%, and 2) this inflection was reversed after the treatment was removed.

Protein Extraction and Western Blotting

MIN6 cells were grown on 6-well plates (Thermo Fischer Scientific; Rochester, NY) to a confluency of 80-90%, then lysed using Cell Signalling Lysis Buffer (Beverly, MA) for CHOP, XBP-1, cleaved caspase 3, 9, and 12 or Cell Signalling Lysis Buffer supplemented with phosphatase inhibitors (50 mM sodium fluoride, 10 mM sodium pyrophosphate decahydrate, and 10 mM β-glycerophosphate) for phosphorylated PERK and phosphorylated eIF2α. The cells were then sonicated for 30 seconds and cleared by centrifugation at 10,000 rpm for 5 to 15 minutes. Protein concentrations were determined via BCA assay (Pierce; Rockford, IL) and samples were loaded onto SDS-PAGE gels. Separated proteins were transferred onto PVDF membranes via a semi-dry transfer apparatus and blocked using I-Block (Tropix; Bedford, MA), containing 0.1% Tween-20. All primary antibody incubations were done overnight at 4°C except for rabbit monoclonal phosphorylated PERK and phosphorylated eIF2α primary antibodies (Cell Signalling; Boston, MA) which were incubated over 48 hours at 4°C. Secondary antibodies were incubated at room temperature for one hour in I-Block containing 0.1% Tween-20.

Data Analysis

All studies were replicated at least 3 times. Results are presented as means plus or minus standard error of the means. Statistical analysis was performed as indicated in the text. Unpaired, two-tailed t-tests and one-way ANOVA with Tukey's post-hoc analyses were used where appropriate. A p value of <0.05 was considered significant.

Chapter Three: Results

Acute effects of palmitate on cytosolic Ca^{2+}

Palmitate is known to stimulate Ca^{2+} signals in some β-cell models (118, 129), but these Ca^{2+} signals have not been fully characterized. Previous data using human islet β-cells indicated that robust and complex cytosolic Ca^{2+} signals occurred in response to 100 μM palmitate (53). To further characterize the mechanisms of these responses we employed the MIN6 β-cell line, which is homogenous, readily available, and can be easily transfected with cameleon DNA. Many reports use different concentrations of palmitate, so a dose-response experiment was performed using MIN6 cells loaded with the cytosolic Fura-2-AM dye. Example traces of each dose, ranging from 25 μM to 500 μM palmitate, are shown (**Fig. 3**). Palmitate was coupled to BSA in a 6:1 ratio in all experiments (90), which is a physiological ratio of palmitate:BSA in the obese state (117). Normal plasma free fatty acid levels, which are lower in lean individuals, exist closer to a 2:1 free fatty acid:BSA ratio (24). The average cytosolic Ca^{2+} response was analyzed over this concentration range (**Fig. 3**), indicating no significant differences between the concentrations. These experiments demonstrate that palmitate induces a significant number and amplitude of responses at the lowest concentration tested.

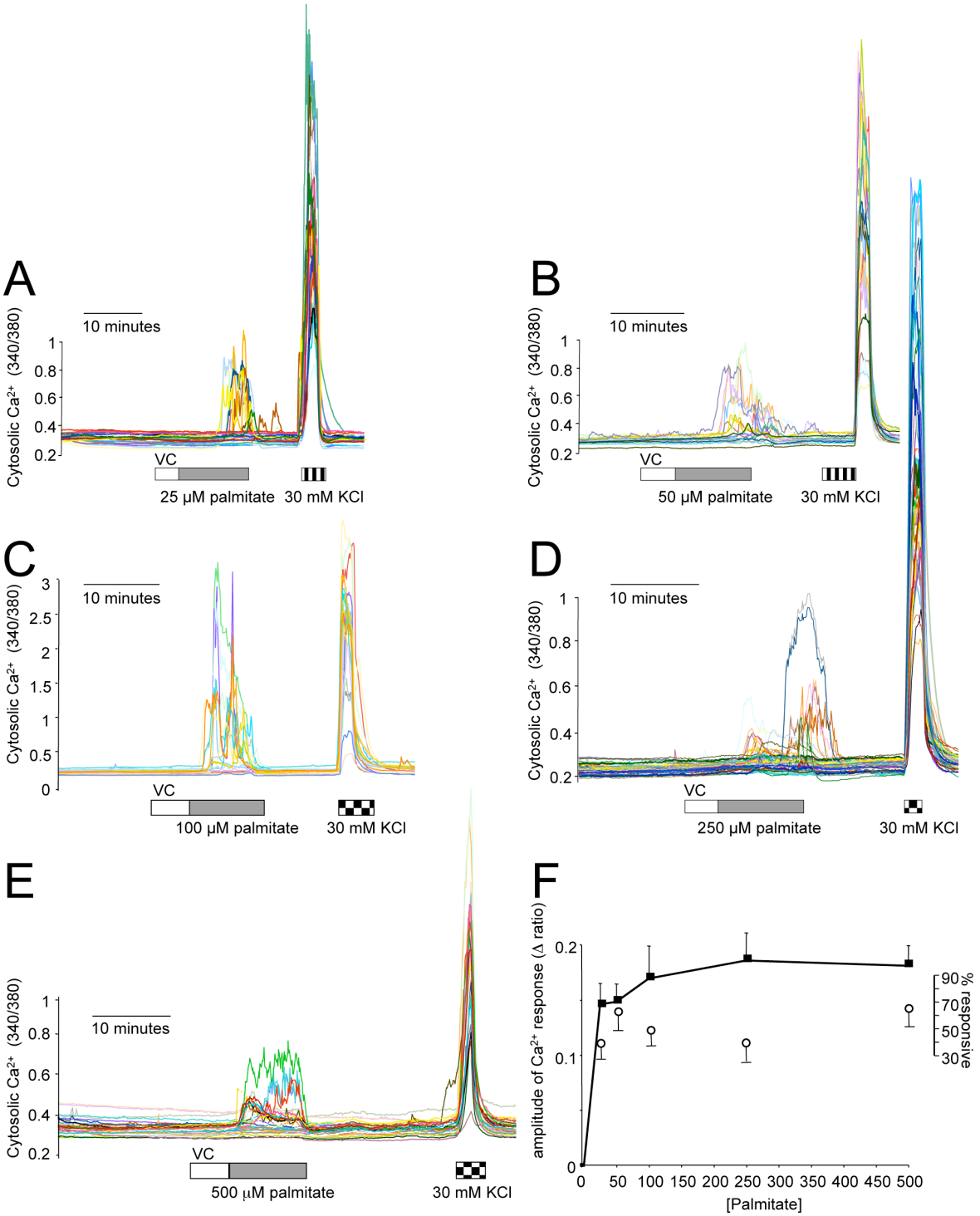

Figure 3. Palmitate Ca^{2+} dose-response in MIN6 cells. (**A-E**) Representative traces of all cells from different days are shown. Cytosolic Ca^{2+} concentration was measured using Fura-2-AM dye. Each does represents n=3-4. The total number of cells measured for each concentration was 44 (25 μM), 66 (50 μM), 56 (100 μM), 90 (250 μM), and 62 (500 μM). All solutions were made with a 6:1 ratio of palmitate: BSA, and the baseline solution contained 3 mM glucose and 0.1% BSA. (**F**) Quantification of the dose-response. The response was analyzed by the average amplitude of the Fura-2 Ca^{2+} signal (left axis), and the percent of cells responsive to palmitate (right axis).

D3cpv cameleon captures acute cytosolic Ca^{2+} signals induced by palmitate

In addition to its ability to acutely stimulate β-cells, palmitate has potent long-term effects on β-cell function and survival. To determine the effects of sustained palmitate exposure on β-cell Ca^{2+} homeostasis, the recently developed FRET-based cytosolic Ca^{2+} indicator, D3cpv, was employed to follow cytosolic Ca^{2+} patterns under extended palmitate treatment. This genetically-encoded cameleon allowed for long-term Ca^{2+} imaging experiments, in contrast to Fura-2 dye, which performs poorly over long periods of time (>1 hour) due to dye leakage, dye compartmentalization into organelles, and photo-bleaching. First, the relative sensitivity for measuring palmitate-induced signals between the D3cpv cameleon and Fura-2-AM dye was determined. As expected, the D3cpv FRET probe recorded the characteristic cytosolic Ca^{2+} signals evoked by acute exposures to 20 mM glucose, as well as 100 μM palmitate and 25 mM KCl in MIN6 cells (**Fig. 4**). Together, these experiments indicated that D3cpv is an effective Ca^{2+} probe for β-cells and that it accurately captured the palmitate-induced Ca^{2+} signals that have been previously characterized using other methods.

Mechanisms of palmitate-induced Ca^{2+} signals

To identify the sources of the palmitate-induced cytosolic Ca^{2+} signals, β-cells were perifused with Ca^{2+}-free buffer to test whether extracellular Ca^{2+} was required. In MIN6 β-cells, palmitate caused a transient Ca^{2+} signal but not a sustained Ca^{2+} elevation in the absence of extracellular Ca^{2+} (**Fig. 5**), similar to data obtained using human β-cells (53). Additionally, removing extracellular Ca^{2+} inhibited palmitate-induced Ca^{2+} signals that had already been initiated (**Fig. 5**). These results demonstrate that palmitate can initiate Ca^{2+}

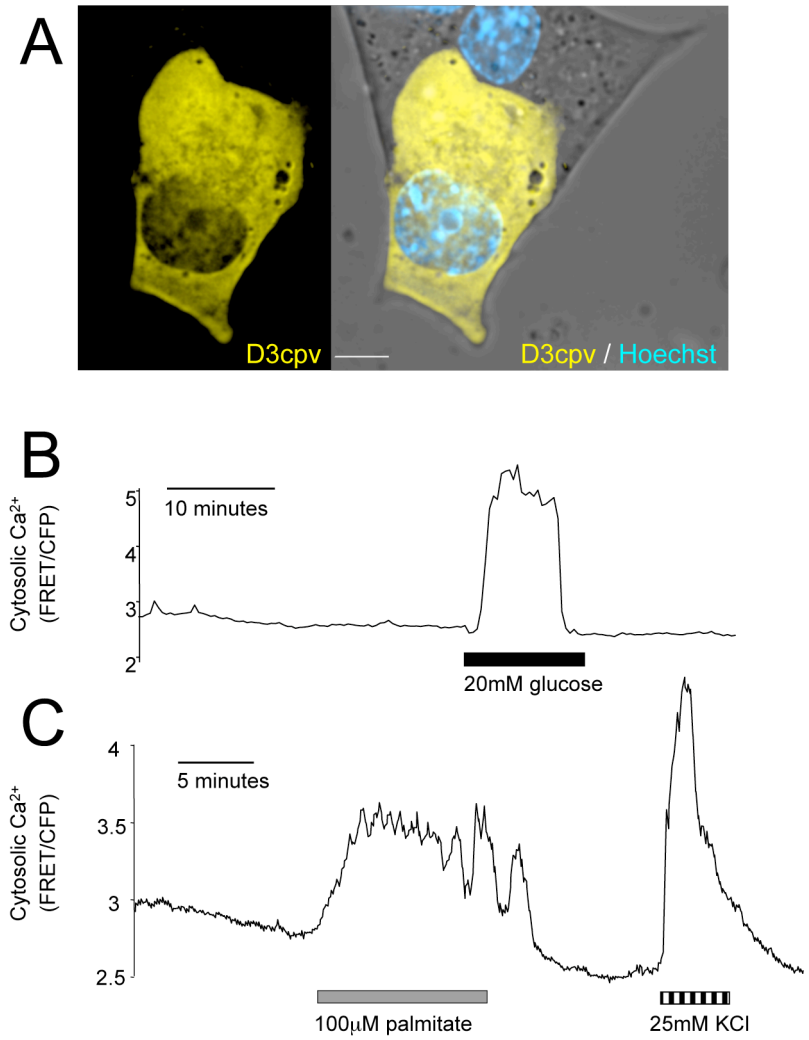

Figure 4. FRET-based cytosolic Ca^{2+} imaging of palmitate signalling. (**A**) The cytoplasm-targeted FRET cameleon D3cpv. Nuclei are counterstained with Hoechst 33342 dye. Scale bar is 5 μm. (**B**) MIN6 cells expressing D3cpv exposed to 20 mM glucose (n=13 cells). Ca^{2+} concentration is shown as a ratio between FRET emission and CFP fluorescence of the cytosol-targeted construct. (**C**) MIN6 cells expressing D3cpv sequentially exposed to 100 μM palmitate and 25 mM KCl (n=21 cells).

signals in the absence of extracellular Ca^{2+}, but that Ca^{2+} influx from the extracellular space is required for continued propagation of palmitate-induced Ca^{2+} signals. Importantly, these findings implicate intracellular Ca^{2+} stores as a component of fatty acid-induced Ca^{2+} signalling, in agreement with studies using other β-cell models (118, 129).

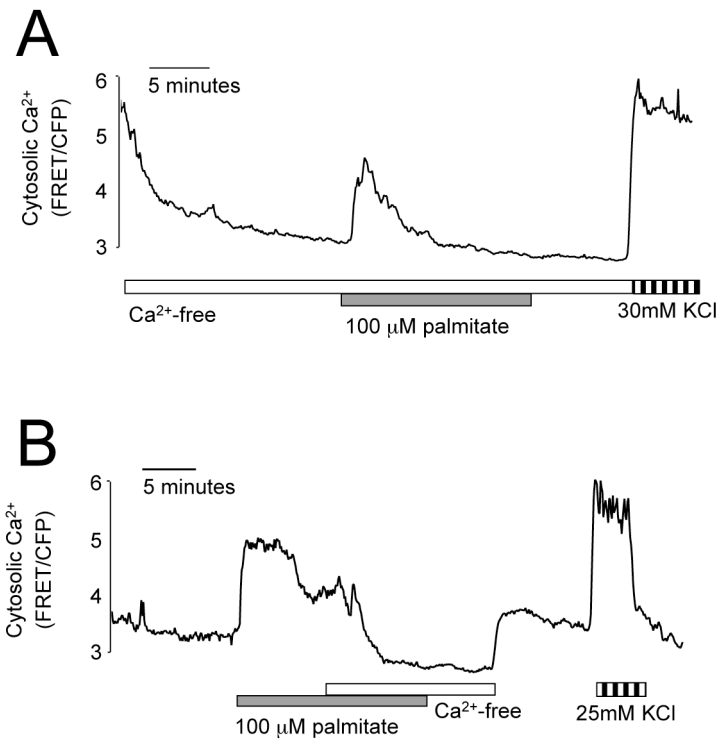

Figure 5. Mechanisms of palmitate-induced cytosolic Ca^{2+} signals in MIN6 cells. (**A**) Effects of pre-treatment with extracellular Ca^{2+} free solution on palmitate-induced Ca^{2+} signals in MIN6 cells. (**B**) Removal of extracellular Ca^{2+} during the response to palmitate blocked the sustained oscillations in MIN6 cells. Representative traces are shown (A, n=12 cells; B, n=21 cells).

The long-chain free fatty acid receptor, GPR40, can be activated by palmitate and has been suggested to generate intracellular Ca^{2+} signals through PLC-mediated IP_3 generation in β-cells (15, 60). To determine the extent to which IP_3 receptors are involved in this intracellular Ca^{2+} store release, cells were treated with palmitate in the presence of xestospongin C, a drug that blocks IP_3 receptors (IP_3R) (66). MIN6 cells were pre-treated with 1 μM xestospongin C for 10 or 20 minutes and the area under the curve of the initial (first phase) and sustained (second phase) of the palmitate-induced Ca^{2+} signals was quantified (**Fig. 6**). The first minute of response was expected to involve intracellular stores, and xestospongin C tended to reduce the 1st phase of the palmitate-induced Ca^{2+} signals. However, this difference did not reach statistical significance despite a large number of cells

studied. This result suggests that the IP_3R may not play a dominant role in palmitate-induced intracellular store Ca^{2+} release, or that the dose of drug, duration of treatment, was too low to fully inhibit signal transduction.

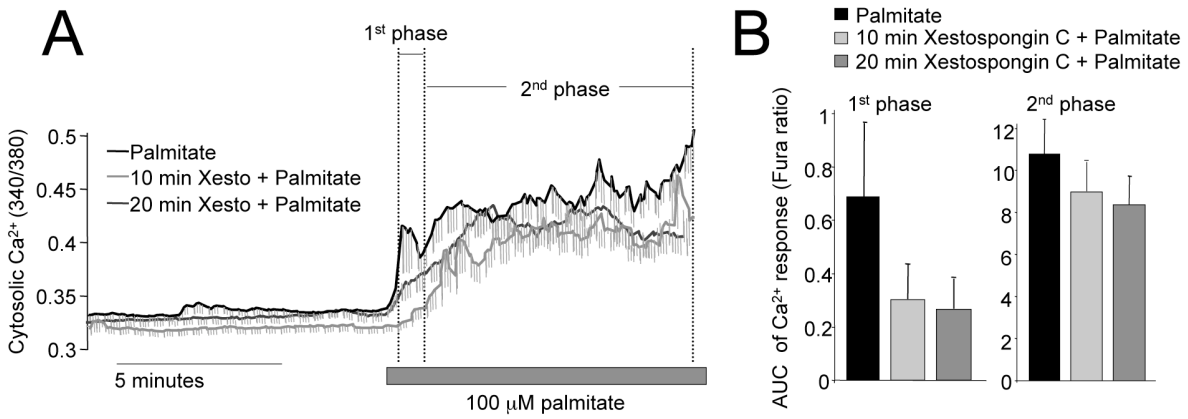

Figure 6. Blocking IP_3R does not block palmitate-induced cytosolic Ca^{2+} signals. (**A**) Effects of 10 or 20 minute pre-treatment of 1 μM Xestospongin C on palmitate-induced cytosolic Ca^{2+} signals in Fura-2-AM loaded MIN6 cells. The first and second phases of the Ca^{2+} response are indicated. (**B**) AUC quantification of the first and second phases of the Ca^{2+} response. n=43 cells (palmitate alone), 42 cells (10 minute Xestospongin C treatment), 50 cells (20 minute Xestospongin C treatment).

Acute palmitate treatment causes a decrease in ER Ca^{2+}

The ER is thought to be the main dynamic intracellular Ca^{2+} storage compartment in β-cells (39). To dynamically measure Ca^{2+} levels in the ER lumen of MIN6 cells, the recently developed targeted cameleon probe was used (105, 106). This genetically engineered indicator has Ca^{2+}-responsive elements between an enhanced cyan fluorescent protein (eCFP) and the citrine yellow fluorescent protein variant (**Fig. 2**). FRET between these fluorescent proteins changes upon Ca^{2+} binding to the probe (105). Acute palmitate treatment caused a reversible decrease in ER Ca^{2+}, in a subset (31.3 ± 4.7%) MIN6 cells (**Fig. 7**; 114 responsive cells of 476 cells measured in total). These Ca^{2+} signals were also repeatable within individual cells (**Fig. 7**). To determine the extent of this depletion, the

decrease in ER Ca^{2+} caused by palmitate was compared to that caused by thapsigargin (1 μM), a drug that directly inhibits the SERCA Ca^{2+} uptake pumps on the ER. In the palmitate-responsive MIN6 cell subset, the fatty acid depleted ER Ca^{2+} to a level that was 45 ± 3.7% of that caused by thapsigargin, which affected all cells (**Fig. 7**). In a limited number of preliminary experiments, blocking IP_3R with 1 μM xestospongin C did not block palmitate-induced ER Ca^{2+} release in MIN6 cells (**Fig. 8**), suggesting that IP_3 generation is not necessary for the palmitate response. Further, treatment of MIN6 cells with the non-metabolizable palmitate analogue 2-bromopalmitate did not consistently stimulate a robust release of ER Ca^{2+} (**Fig. 9**; n = 83 cells), suggesting that palmitate metabolism is required for this effect. Together, these data provide a direct demonstration that ER intracellular Ca^{2+} store mobilization plays a role in palmitate-induced Ca^{2+} signalling.

Effects of oleate on ER Ca^{2+} dynamics

The monounsaturated fat oleate has been shown to affect β-cells in a number of studies, although it is generally considered to be less toxic (31, 38, 49, 68, 85, 86). Oleate is thought to activate GPR40 in β-cells (46, 129). In D1ER-transfected MIN6 cells, oleate caused a decrease in ER luminal Ca^{2+} that was similar to that of palmitate (**Fig. 10**). There was a trend that a higher percentage of cells responded to oleate (45± 8% for oleate, 25±5% for palmitate; not statistically significant; **Fig. 10**). This may be a dose-dependent effect, as the free concentration of oleate in equilibrium with its BSA-bound form is twice that of palmitate (120). Alternatively, if this signal is initiated by GPR40 activation, oleate has been shown to have a higher affinity for GPR40 than palmitate (60). In experiments where these fatty acids were added sequentially, there was no difference in response to either fat after

treatment with the other (**Fig. 11**). Together, these results indicate that palmitate does not block the cell's ability to respond to oleate, and that oleate also does not seem to impair the ability of palmitate to signal

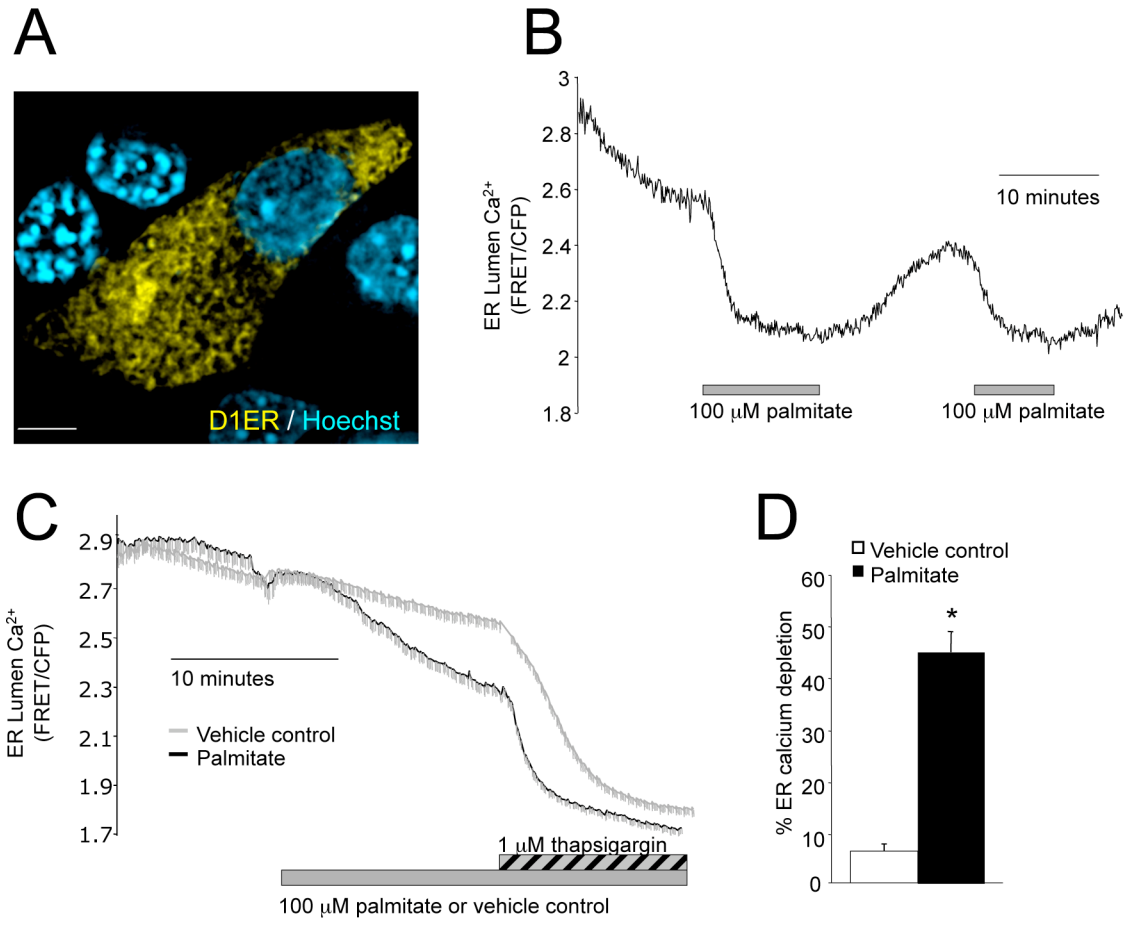

.

Figure 7. Direct imaging of ER luminal Ca^{2+} in palmitate-treated MIN6 cells. (**A**) The endoplasmic reticulum-targeted Ca^{2+} sensor D1ER. The nuclear dye, Hoechst 33342, was added to live cells for contrast. Scale bar is 5 μm. (**B**) Live cell imaging with D1ER revealed that 100 μM palmitate acutely and reversibly decreased ER Ca^{2+}. The trace is representative of 12 responding cells out of 66 total cells imaged. (**C,D**) Comparison of palmitate-induced ER Ca^{2+} release to 1 μM thapsigargin. (**C**) Representative average trace of cells treated with 100 μM palmitate or vehicle control then stimulated with 1 μM thapsigargin. (**D**) Quantification of the decrease in ER Ca^{2+} induced by palmitate compared to that of thapsigargin. n=3 experiments done on different days; palmitate cells = 20-23, and control cells = 54-68 each experiment. The baseline solution for all experiments contained 3 mM glucose. * denotes significance over control (p<0.05).

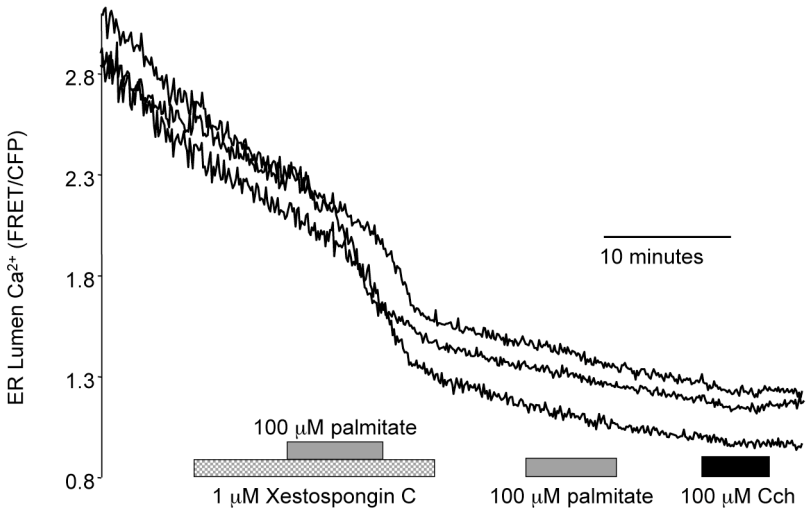

Figure 8. Blocking IP_3R does not block palmitate-induced ER Ca^{2+} release. MIN6 cells transfected with D1ER were pre-treated with 1 μM Xestospongin C and then exposed to 100 μM palmitate. Representative traces from three cells are shown. 16 cells were imaged in total, with 10 cells responding to palmitate in the presence of the drug.

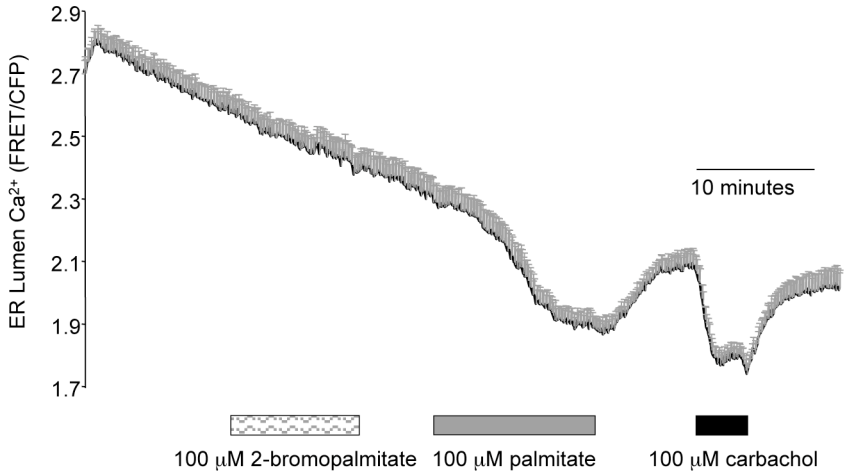

Figure 9. 2-bromopalmitate does not initiate ER Ca^{2+} release. MIN6 cells transfected with D1ER were exposed to 100 μM 2-bromopalmitate followed by 100 μM palmitate and 100 μM carbachol. The average trace of 10 palmitate-responding cells is shown. 88 cells were imaged in total and no cell responded to 2-bromopalmitate. The baseline solution contained 3 mM glucose and 0.1% BSA.

Long-term analysis of Ca^{2+} signals using cameleons

A major advantage of the fluorescent protein-based Ca^{2+} indicators is their utility in long-term experiments. In this study, experiments were done examining cytosolic and ER Ca^{2+} responses to palmitate in MIN6 cells over multiple hours. Interestingly, palmitate-

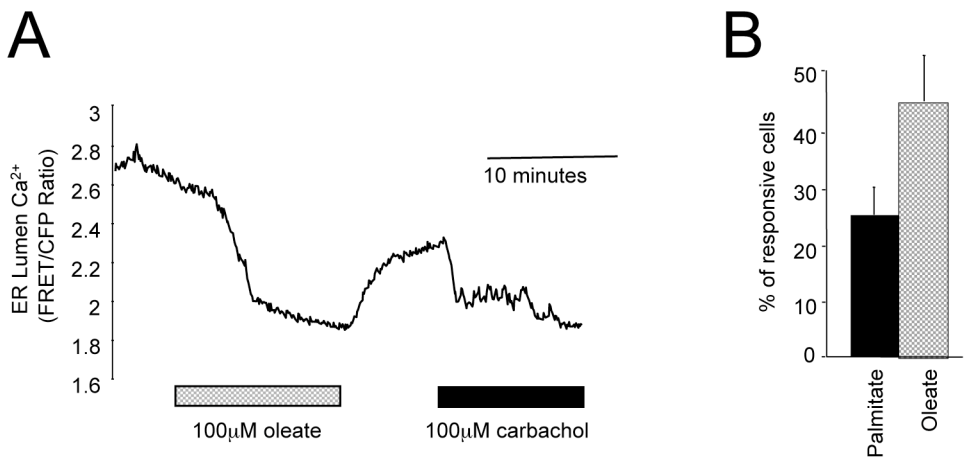

Figure 10. Oleate mobilizes ER Ca^{2+} stores. (**A**) Treatment of D1ER-transfected MIN6 cells with 100mM oleate (6:1 BSA) evoked a similar response in ER calcium release to that caused by palmitate. Shown is a representative trace of 35 cells out of 125 cells imaged. (**B**) Quantification of the overall fatty acid responses in D1ER-transfected MIN6 cells (oleate compared to experiments done with palmitate).

induced cytosolic Ca^{2+} oscillations were sustained and did not appear to diminish appreciably with time in a large proportion of cells (**Fig. 12**). This indicates that in the continuous presence of palmitate, the fatty acid generates signals using components that do not desensitize within the time frame of these studies. Additionally, there were distinct groups of cellular responses to palmitate. About half of the cells responded immediately, and ~75% of these exhibited sustained cytosolic Ca^{2+} oscillations (**Fig. 12**). The other half of cells did not begin responding with sustained cytosolic Ca^{2+} oscillations until they had been exposed to palmitate for an average of ~50 minutes. No signals were observed under baseline conditions (3 mM glucose with vehicle control) (**Fig. 12**). Additionally, ER Ca^{2+} depletion upon long-term palmitate stimulation was also observed (**Fig. 12**). Typically, palmitate induced release of ER luminal Ca^{2+} that included a gradual and oscillatory refilling of the organelle (**Fig. 12**). Furthermore, these cells remained responsive to 100 μM carbachol, an IP_3-generating agonist, after 100 minutes of palmitate treatment. Together,

these results demonstrated that SERCA pumps were still active and the ER Ca^{2+} store was not completely and permanently depleted in the prolonged presence of palmitate.

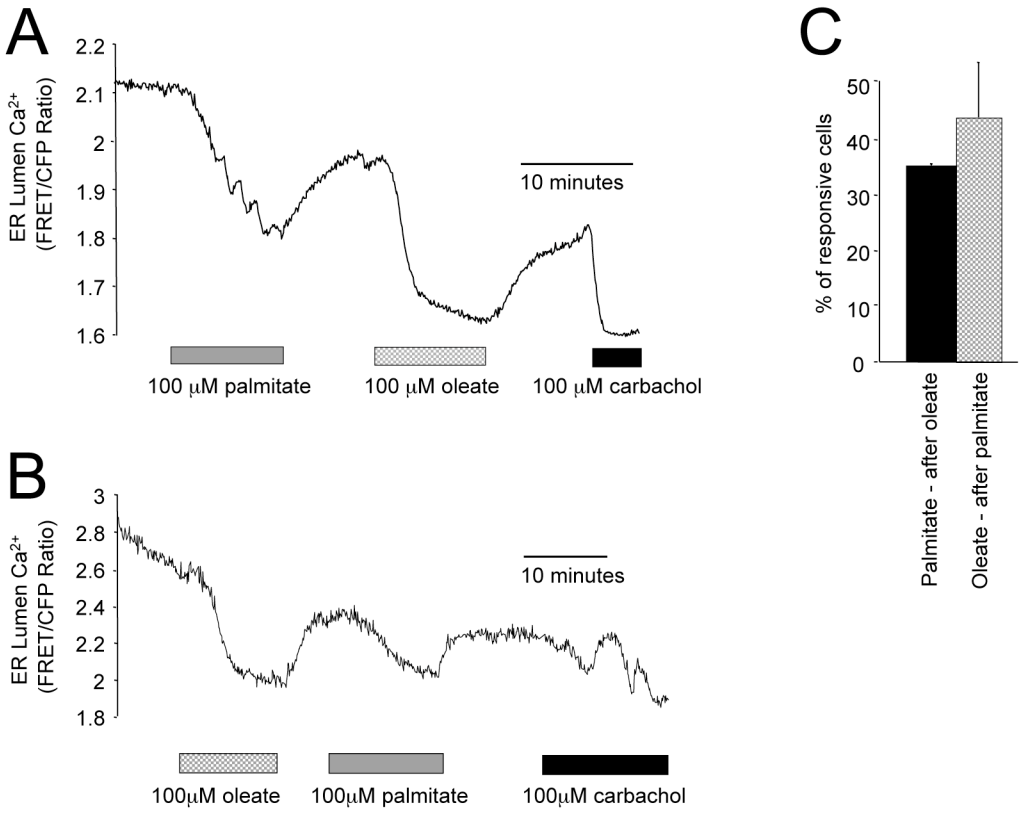

Figure 11. Oleate does not block palmitate's ability to mobilize ER Ca^{2+} stores. (**A, B**) When one fatty acid was applied first, there was no different between the response rate compared to the other fat. (**A**) Treatment of D1ER-transfected cells with 100 μM palmitate followed by 100 μM oleate (n= 22 out of 86 cells), and the converse (**B**) (n=15 out of 99 cells) revealed similar signals evoked by the two fatty acids that did not cause a block of the signal when applied first. 100 μM carbachol is used as a positive control for cells with responsive IP_3R activation. Representative traces are shown, n=3-4 of different days of experimentation. (**C**) Quantification of overall responses revealed no difference in fatty acid responses.

Effect of chronic treatment of palmitate on Ca^{2+} dynamics

In previous studies of β-cells chronically treated with palmitate, indirect measurements of Ca^{2+} store loading yielded conflicting results (26, 68). To directly test the hypothesis that chronic palmitate treatment alters ER Ca^{2+}, ER Ca^{2+} was measured in D1ER-

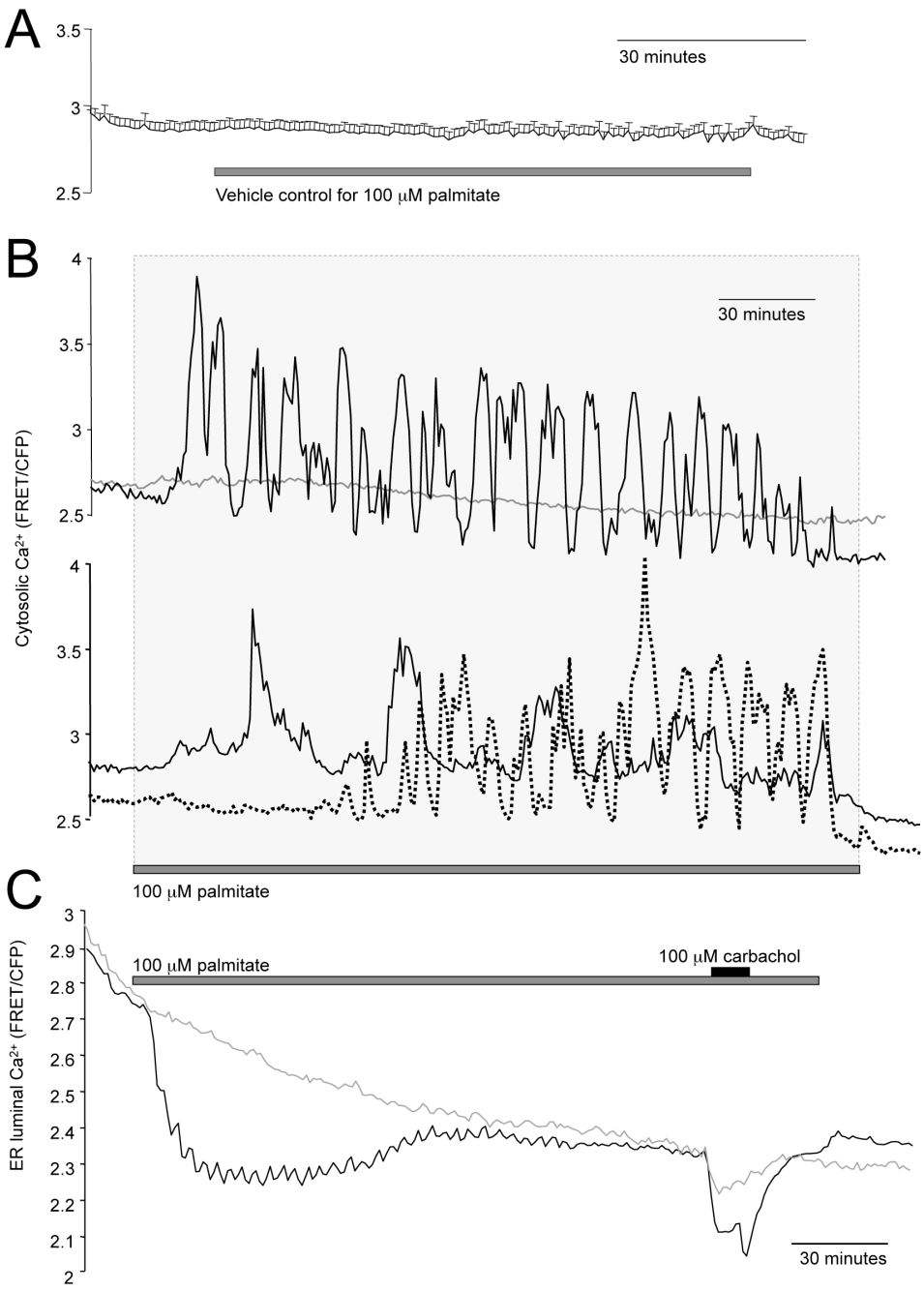

Figure 12. Long-term imaging of palmitate-induced Ca^{2+} dynamics. (**A**) Average of vehicle-control treated D3cpv-expressing MIN6 cells; all cells were KCl-responsive (n=11 cells). (**B**) Heterogeneous, oscillatory cytosolic Ca^{2+} responses to palmitate with long-term exposure. Three classes of responses were observed (transient, continuous oscillations, delayed oscillations) in D3cpv-expressing MIN6 cells treated with 100 μM palmitate. Representative traces are shown (n= 44 cells). (**C**) Long-term imaging of ER Ca^{2+} depletion in response to 100 μM palmitate and 100 μM carbachol in D1ER-expressing MIN6 cells. A representative trace is shown (n=57 cells). Non-responding cells are shown in (B,C) to demonstrate the typical photobleaching-associated signal loss.

transfected MIN6 cells exposed to palmitate for 24 hours in low glucose conditions (5 mM). Baseline ER Ca^{2+} levels were significantly lower in the palmitate-treated cells compared to the vehicle control-treated cells (**Fig. 13**). The amount of ER Ca^{2+} that could be released upon thapsigargin treatment was not significantly different, suggesting that chronic palmitate exposure did not affect the thapsigargin-sensitive pool of ER Ca^{2+}. These results indicate that chronically high levels of palmitate may affect the ER Ca^{2+} 'set-point' and contribute to deregulation of β-cell Ca^{2+} homeostasis.

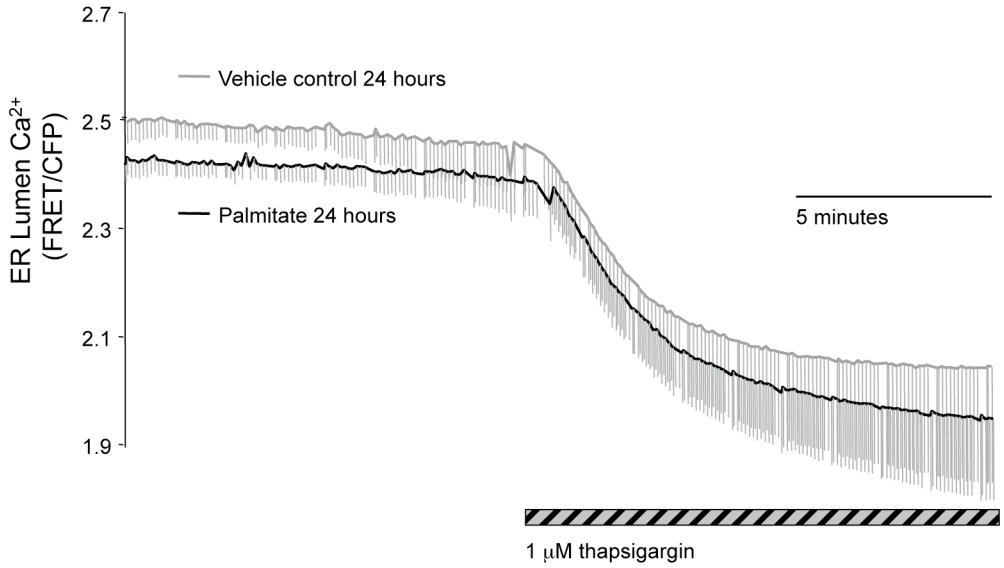

Figure 13. Effect of chronic palmitate treatment on ER Ca^{2+} dynamics. MIN6 cells transfected with D1ER were treated with 1500 μM palmitate (6:1 BSA) or vehicle control in 5mM glucose for 22-25 hours and ER Ca^{2+} was measured, with the addition of 1 μM thapsigarin. The trace shown is an average of 3 coverslips each of palmitate-treated cells (111) and control cells (77).

Characteristics of ER stress and caspase activation in β-cells

Changes in ER Ca^{2+} levels can lead to chaperone dysfunction, an increase in misfolded proteins, and subsequent initiation of the ER stress response (130). Using pharmacological agents that induce ER Ca^{2+} depletion, the time-course of signalling events that mediate ER stress was analyzed. Thapsigargin (1 μM) and carbachol (100 μM) together

resulted in a rapid and homogeneous depletion of the ER Ca^{2+} stores, compared to either drug alone (81). The pro-apoptotic transcription factor CHOP and the death effector Capsase 3 were both activated upon chronic thapsigargin treatment (81). To elucidate the signals that may link ER Ca^{2+} depletion to downstream ER stress and apoptosis signals, the PERK/eIF2α arm of the ER stress pathway was characterized. PERK was rapidly phosphorylated within 5 minutes of thapsigarin treatment (**Fig. 14**), and this subsequently lead to eIF2α phosphorylation. Both PERK and eIF2α remained activated for the duration of the treatment, up to 4 hours (**Fig. 13**). This effect was not exacerbated by the additional treatment with carbachol. These kinetics implicate that rapid perturbations of ER Ca^{2+} homeostasis can lead to an immediate and sustained ER stress response, which under some circumstances can then lead to caspase 3 activation and apoptosis (81).

To further characterize the effect of ER Ca^{2+} perturbation on apoptosis signalling, the activation of caspases 7 and 9 was examined. Similar to what was seen with capsase 3 cleavage (81), both caspases 7 and 9 were strongly up-regulated after chronic thapsigargin treatment (**Fig. 15**). Treatment with drugs that block ER Ca^{2+} release from IP_3R (xestospongin C) and RyR (ryanodine) channels did not significantly allay the apoptosis signals in these experiments (**Fig. 15**). Taken together, these results demonstrate that chronic disruption of ER Ca^{2+} levels leads to a sustained ER stress response, which then causes β-cell death.

Effects of palmitate on ER stress

Sustained elevations in intracellular Ca^{2+} are known to predispose β-cells to programmed cell death. Moreover, extended periods of lowered ER Ca^{2+} also promote the

induction of ER-stress and cell death (81). Given the rapid effects of palmitate on luminal

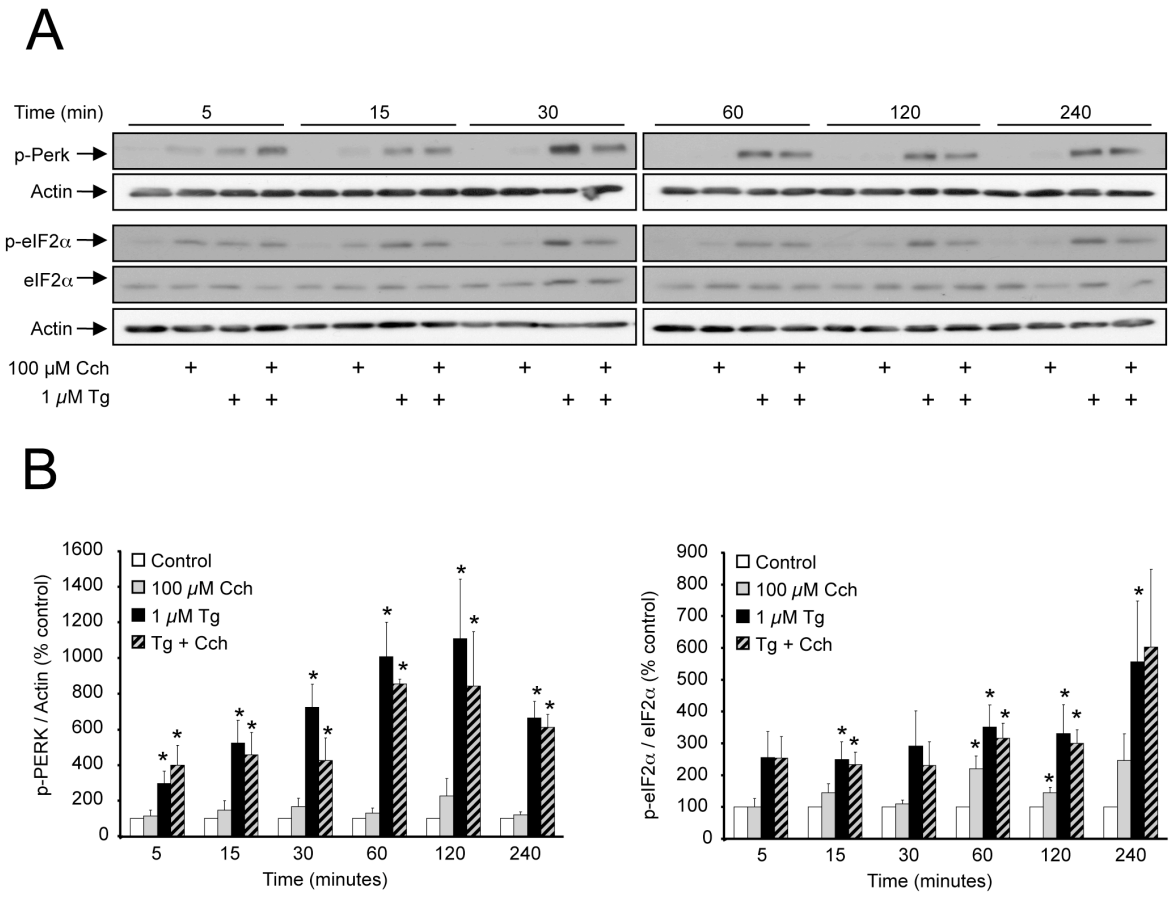

Figure 14. Effects of IP_3R activation on UPR activation evoked by SERCA inhibition. (**A**) Phosphorylation of PERK and eIF2α in 25 mM glucose cultured MIN6 cells was examined at the time points indicated. (**B**) Quantification of western blots for PERK and eIF2α phosphorylation. (Similar results from experiments conducted in 5 mM and 25 mM glucose were pooled; n=6). * denotes significance over control (p<0.05). Cch, carbachol; Tg, thapsigargin.

ER Ca^{2+}, palmitate may also activate the components of the ER-stress response rapidly. Indeed, in MIN6 cells treated with palmitate, in the presence of 5 mM glucose, there was a significant increase in the phosphorylation of luminal ER Ca^{2+} sensor PERK, after just 5 minutes (**Fig. 16**). The other arm of the ER stress signalling cascade is initiated by activation of IRE1, and results in the splicing and activation of the transcription factor XBP-1 (130). Extended palmitate treatment tended to cause a increase in the activated, spliced (54kD)

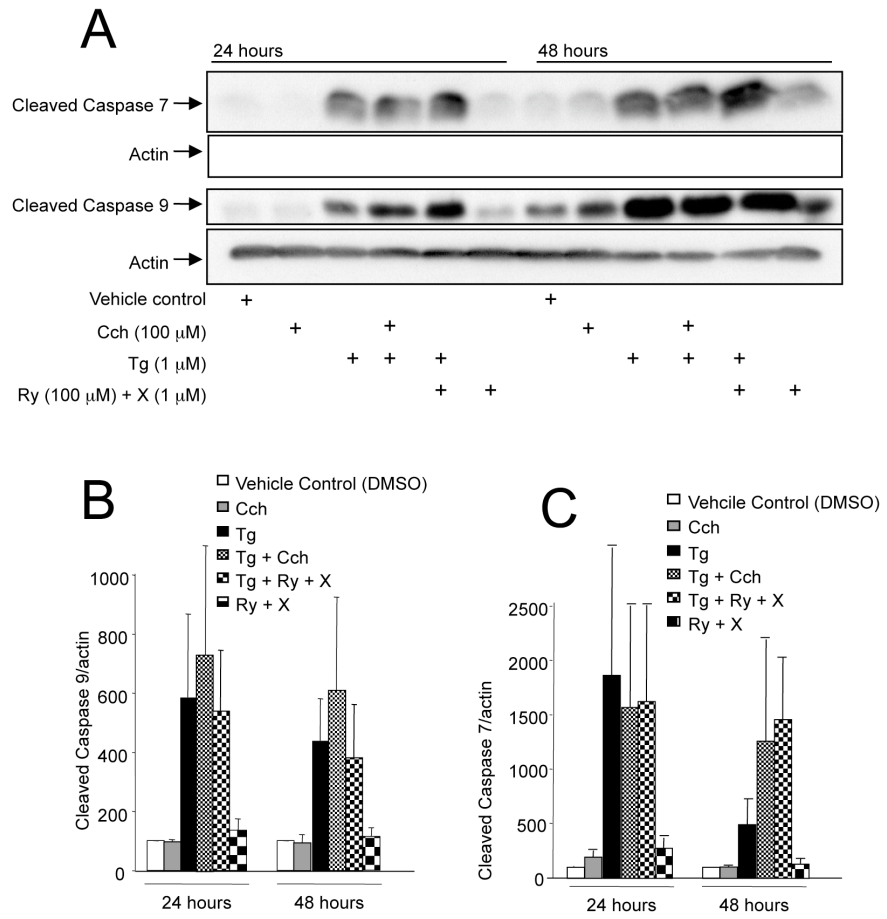

Figure 15. Blocking ER Ca^{2+} release does not attenuate thapsigarin-induced caspase actiavtion. (**A**) Caspase 7 and caspase 9 activation in MIN6 cells upon treatment with carbachol (Cch), thapsigargin (Tg), ryanodine (Ry) or Xestospongin C (X) at the time-points indicated. (**B,C**). Quantifications of the western blots for caspase cleavage.

form of XBP-1 (77) (**Fig. 17**), which also coincided with the activation of the pro-apoptotic transcription factor CHOP (53), consistent with previous reports (23, 68, 70, 77). This also correlated with the kinetics of palmitate-induced propidium iodide incorporation, an indicator of β-cell death (53). Blocking the release of ER IP_3R- and RyR-gated Ca^{2+} stores using xestospongin C and ryanodine concomitantly with palmitate treatment did not decrease the activation of XBP-1 (**Fig. 17**). Blocking extracellular Ca^{2+} influx through L-type Ca^{2+} channels with nifedipine also failed to block palmitate-induced XBP-1 activation

at 12 hours, but did mitigate palmitate's effect at 24 hours of treatment (**Fig. 17**). Together, these results indicate that palmitate treatment in low glucose conditions does indeed initiate a sustained ER stress response mediated in part by ER Ca^{2+} store mobilization. However, this modification in Ca^{2+} homeostasis alone is not likely to be sufficient to maintain ER-stress or initiate β-cell apoptosis.

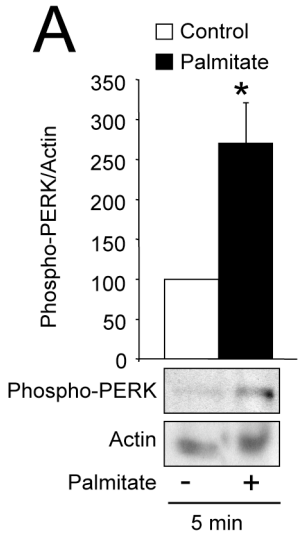

Figure 16. Palmitate induces acute PERK phosphorylation. (**A**) Levels of phospo-PERK after short (5 minutes) treatment with 1500 μM palmitate (6:1 palmitate to BSA), after 6 hours of culture in low (5 mM) glucose; n=5. * denotes significance over control (p<0.05).

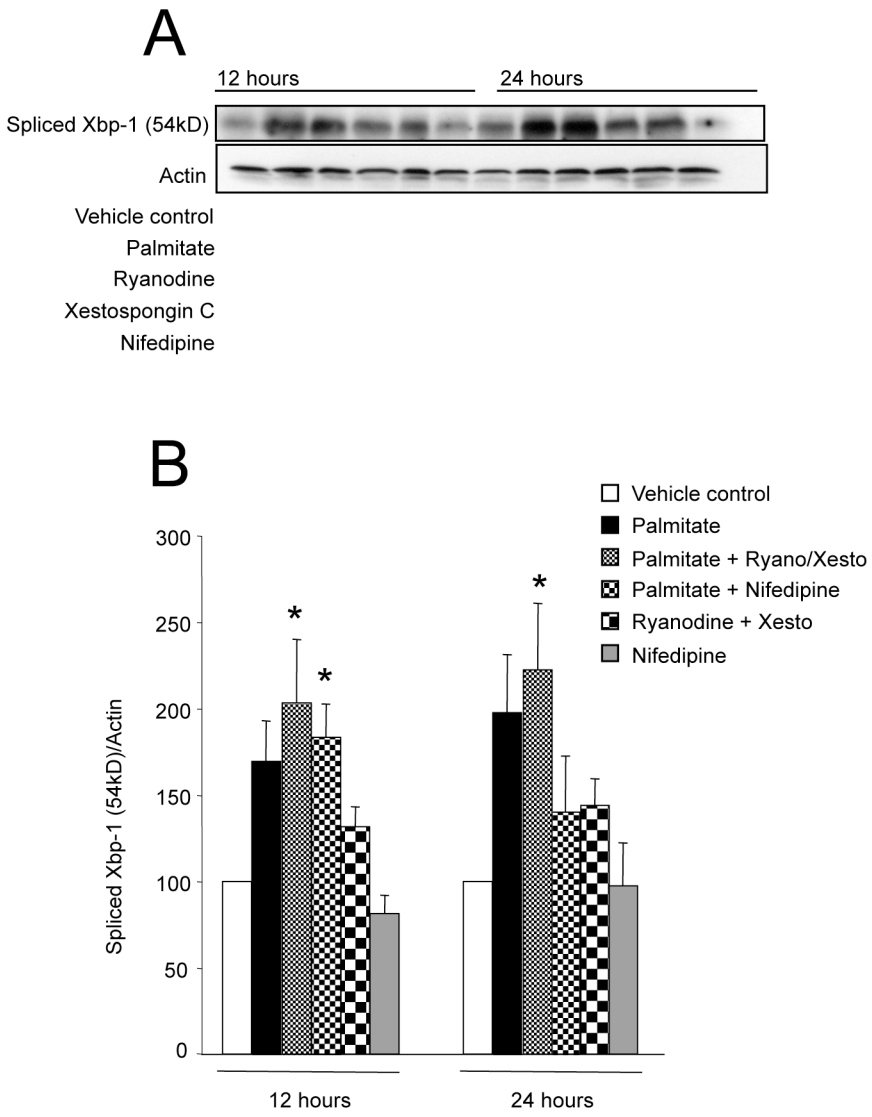

Figure 17. Blocking ER Ca^{2+} release does not inhibit palmitate-induced XBP-1 splicing. (**A**) Spliced XBP-1 protein levels after 24-48 hours of treatment with 1500 μM palmitate (6:1 palmitate to BSA) in low glucose (5 mM), n=5-6 with the indicated drugs. (**B**) Quantification, analyzed using a one-way ANOVA and Tukey's post-hoc test. * denotes significance over vehicle control ($p<0.05$).

Chapter Four: Discussion

The objective of this project was to elucidate the effects of palmitate on pancreatic β-cell Ca^{2+} homeostasis. The study has three main findings. First, palmitate caused cytosolic Ca^{2+} signals in MIN6 cells, in agreement with previous findings in other β-cell lines, primary mouse islets, and human β-cells (53, 118, 129). Second, these Ca^{2+} signals were generated by a combination of extracellular Ca^{2+} influx and Ca^{2+} release from intracellular stores: both palmitate and oleate mobilized Ca^{2+} release from the ER lumen. Third, both pharmacological and palmitate-induced Ca^{2+} depletion induced the ER-stress response with rapid kinetics. Together, these findings contribute to the understanding of the mechanisms by which the saturated fatty acid palmitate alters β-cell function.

Palmitate-induced cytosolic Ca^{2+} signals

The nature of the palmitate-induced Ca^{2+} signals in MIN6 cells was characterized in this study. The Ca^{2+} responses were qualitatively and quantitatively similar between MIN6 β-cells and human β-cells (53), indicating that the MIN6 cell line may be a suitable model for studying some aspects of β-cell Ca^{2+} homeostasis. A recent study also described the similarities between MIN6 cells and human β-cells in terms of their susceptibility to apoptosis in response to palmitate (74), but no study has directly compared the two cell types with respect to their palmitate-induced Ca^{2+} responses. In MIN6 cells, even low doses of palmitate (e.g. 25 μM) effectively stimulated cytosolic Ca^{2+} signals. This low dose nevertheless reflects a free (unbound) nanomolar amount of palmitate (120), which is within the normal physiological range for plasma free fatty acids (135). Indeed, experiments done

using an increasing amount of BSA (> 0.1%) demonstrated an inhibition of FFA-mediated signal at high BSA levels, indicating that it is the unbound form of the fatty acid that is the active signalling molecule (46, 60). There have been a wide range of palmitate concentrations used to model lipotoxicty, and indeed, increasing palmitate concentration increases levels of cell death (53, 85). However, in one study a sub-toxic concentration of palmitate did not induce death but did have effects on mitochondrial membrane potential in MIN6 cells (72). This indicates that even low doses of palmitate, which may be the more relevant (and healthy) physiological levels of the fatty acid, induce signals that may be involved in our observed cytosolic Ca^{2+} signals. It may also be interesting to note that a study characterizing oleate signalling found that oleate induced cytosolic Ca^{2+} signals at concentrations as low as 3 μM (46).

Long-term palmitate-induced cytosolic Ca^{2+} signals

The present study provides the first long-term (> 1 hour) measurements of β-cell calcium homeostasis. We compared the acute palmitate responses measured using D3cpv to those established using Fura-2-AM dye (53, 118, 129). The similarities between the signals validate the D3cpv probe as a reliable method for measuring β-cell Ca^{2+}, and justify its use in long-term experiments. Using the D3cpv and D1ER probes over a 3-hour time period demonstrated that palmitate generates sustained, oscillatory Ca^{2+} signals. It was interesting to find that a nutrient other than glucose can generate sustained cytosolic Ca^{2+} responses. In β-cells, one theory posits that the enzyme phosphofructokinase (PFK) drives oscillatory Ca^{2+} signals in response to glucose metabolism, which in turn drive pulsatile insulin release (37, 100, 154). In contrast, a recent report found that multiple glycolysis-independent metabolites can also generate β-cell Ca^{2+} oscillations, suggesting that PFK, and glycolysis itself, is not

necessary for this oscillatory behavior in β-cells (56). The experiments in our study were done using a sub-stimulatory glucose concentration (3 mM), and no Ca^{2+} signals were observed in these baseline conditions, indicating that palmitate is solely driving the observed Ca^{2+} response. Additionally, because treatment with 2-bromopalmitate, a non-metabolizable analog of palmitate, does not generate cytosolic Ca^{2+} signals like that of palmitate (53), these sustained Ca^{2+} signals may be due to direct palmitate metabolism, perhaps driven by β–oxidation-derived metabolites or by downstream LC-CoA signalling.

Mechanisms behind palmitate-induced ER Ca^{2+} signals

This work sheds new light on the mechanisms underlying the palmitate-induced Ca^{2+} signals. Although some investigators have reported that fatty acids do not reduce thapsigargin-mobilizable Ca^{2+} stores (46, 68), other reports suggested the possible role of both extracellular Ca^{2+} influx and intracellular store release (20, 118). Our data, using MIN6 cells, support the latter model. Importantly, for the first time palmitate-induced ER depletion was directly imaged using the D1ER cameleon probe. Previous studies have suggested a role for GPR40 in driving the observed cytosolic Ca^{2+} signals (46, 60, 129). GPR40, a G-protein-coupled receptor (60), would be expected to mobilize ER Ca^{2+} stores via G_q trimeric G-proteins (15, 60), phospholipase C (46), and IP_3R-gated ER Ca^{2+} release. Indeed, pharmacological small-molecule agonists of GPR40 were found to induce IP_3 formation in GPR40-expressing HEK293 cells (141), and inhibition of $G_{q\alpha}$ blocked palmitate potentiation of glucose-stimulated insulin release in mouse islets (76). However, another report noted that palmitate treatment did not result in an increase in IP_3 content in rat islets (2). In our experiments, we were not able to define a major role for IP_3 receptors using pharmacological inhibition. This may be due to the dose or treatment protocol, or due to the fact that a

majority of the cells (~70%) would not have an ER Ca^{2+} response, but yet may have rapid cytosolic Ca^{2+} responses, thus masking the inhibitory effect. Nevertheless, the result leaves open the possibility that palmitate may act on ryanodine receptors (RyR) or the SERCA pumps in mobilizing ER Ca^{2+}. Indeed, previous studies in different model systems, including pancreatic acinar cells, demonstrated that palmitoyl-CoA, the esterified metabolite of palmitate, could activate RyR channels (19, 43, 47, 48), while another study in the HIT β-cell line suggested an effect of palmitoyl-CoA on SERCA activity (29). Additionally, a previous study outlined the requirement for calpain-10 in palmitate-induced β-cell apoptosis, which is also involved in RyR2-activated apoptosis (65), suggesting a possible role for RyR2 in palmitate's lipotoxic action on β-cells.

To further elucidate the mechanism of palmitate-induced Ca^{2+} signals, experiments were carried out using the non-metabolizable palmitate analog 2-bromopalmitate. This molecule is esterified to 2-bromopalmtiate-CoA but cannot undergo β-oxidation. It also prevents other fatty acids from doing so by blocking carnitine palmitoyl transferase-1, which transports long-chain free fatty acids into the mitochondria (119). Treatment of human islets and MIN6 cells with 2-bromopalmitate caused a significantly attenuated Ca^{2+} signal that, nevertheless, was not fully abolished (53). However, we did not detect a decrease in ER luminal Ca^{2+} upon treatment with 2-bromopalmitate in MIN6 cells. This suggests that 2-bromopalmitate cannot mobilize ER Ca^{2+} stores, possibly indicative of its inability to activate GPR40 or other Ca^{2+} channels. Indeed, the effects of 2-bromopalmitate on GPR40 activation remain controversial (107, 127). The possibility remains that the esterified metabolite of 2-bromopalmitate may partially activate Ca^{2+} channels to create the partial cytosolic response (53). A previous report found that concurrent treatment of palmitate with 2-bromopalmtiate

abolished palmitate-induced Ca^{2+} signals (118), perhaps by blocking a receptor or channel or by preventing the action of downstream palmitate metabolites. Another report noted that treatment of mouse islets with palmitoyl-CoA did not mimic palmitate's actions on islet capacitance and Ca^{2+} currents (101), although Ca^{2+} signals were not directly measured. Together, this set of observations indicates that the non-metabolizable analog of palmitate does not replicate the actions of palmitate on β-cell ER Ca^{2+}, suggesting that native palmitate, with its free acidic group, is required for these signals.

Long-term palmitate-induced ER Ca^{2+} depletion

Long-term experiments also indicated that the palmitate-induced ER Ca^{2+} depletion is transient and tends to have an oscillatory re-filling nature. Whether this oscillatory ER behavior occurs concurrently with the observed cytosolic oscillations is unclear, although a previous report demonstrated that ATP-mediated IP_3 production generated ER Ca^{2+} oscillations that were anti-correlated with their corresponding cytosolic Ca^{2+} oscillations (105). Nevertheless, after the 3-hour palmitate treatment, stimulation by the IP_3-generating agonist carbachol in the presence of palmitate indicated that SERCA pumps were active and able to refill the ER Ca^{2+} store. Experiments comparing SERCA activity with and without palmitate were not performed, leaving open the possibility that palmitate may affect SERCA activity kinetics, but our results do indicate that even under longer-term stimulated conditions, palmitate does not fully inhibit SERCA activity. In contrast, under chronic palmitate treatment in low glucose, the basal ER Ca^{2+} level was affected and was indeed lower compared to control-treated cells. This could reflect the action of chronically elevated palmitate at the level of SERCA activity or expression, similar to the effect of cytokines (18), or be a direct effect of palmitate-induced chronic ER Ca^{2+} depletion. In agreement,

chronic palmitate (56) or palmitoyl-CoA (29) treatment has been reported to affect subsequent oscillatory cytosolic Ca^{2+} behavior in response to glucose and other stimulants, indicating the mechanism behind this effect may be due to palmitate's alteration of ER Ca^{2+} levels.

Oleate-stimulated ER Ca^{2+} signals

The monounsaturated fat oleate also transiently mobilized ER Ca^{2+}, in agreement with previous studies showing effects of this fatty acid on β-cell calcium homeostasis (46, 129). Oleate treatment did not block the ability of subsequent palmitate to induce ER Ca^{2+} release, suggesting that the interaction of each fatty acid with its target may be transient. In agreement, a study in rat α-cells, which also express GPR40 (44), demonstrated that blocking ER stores abolished oleate-induced cytosolic Ca^{2+} signals (45). Evidence for a GPR40-mediated mechanism is given through RNAi-mediated GPR40 knockdown studies in rat islets (46) and INS-1 cells (129): the knockdown abolished oleate-stimulated Ca^{2+} signals. However, oleate-stimulated cytosolic Ca^{2+} signals were also demonstrated in cells expressing L-type calcium channels but not GPR40 (145). Palmitate's effects on L-type calcium channels in mouse islets have also been documented (101), suggesting that palmitate may act through these channels as well. These previous studies, in concert with the present one, suggest that fatty acids as well as their metabolites may interact with more than one Ca^{2+} signalling component. Importantly, these studies together with ours suggest that the observed protection offered by oleate against palmitate lipotoxicity (85, 86) does not involve acute ER Ca^{2+} store mobilization.

A similar pattern of oleate's acute vs. chronic effects was shown in a recent study looking at mitochondrial permeability transition (MPT) in MIN6 cells. Acute treatments

with palmitate and oleate both induced similar MPT, but long-term oleate treatment did not induce MPT to the extent of long-term palmitate treatment, and prevented palmitate's induction of MPT when the two fatty acids were co-administered (72). Mitochondrial dysfunction has been documented in lipotoxicity (87), possibly due to the dysregulation in ER integrity, and this study parallels ours in demonstrating oleate's acute, but less chronically toxic, effect.

Glucose-dependence of palmitate Ca^{2+} signals

In the present study, we observed substantial heterogeneity in Ca^{2+} signals induced by palmitate. This is similar to the well-described response heterogeneity seen with glucose (71, 148, 149, 151) and other agonists (66). Notably, we observed only a subset of MIN6 cells (~30%) that responded to palmitate treatment by a reduction in ER Ca^{2+}. It is possible that a higher percentage of MIN6 cells might have responded to palmitate treatment at increased glucose levels. Previous reports have also suggested a glucose-dependence of fatty acid-induced Ca^{2+} signals in mouse (118) and rat β-cells (46). Remizov *et al* (118) suggested that this may be related to increased mitochondrial activity and inhibition of CPT-1 at stimulatory glucose levels, creating a backlog of cytosolic esterified fatty acids which might then become available for signalling. Nevertheless, we observed both cytosolic Ca^{2+} signals and ER Ca^{2+} store mobilization at baseline glucose levels in response to palmitate, providing strong evidence that elevated glucose is not essential for the formation of at least some of these signals.

Kinetics of ER stress and death in β-cells

As dedicated high-capacity secretory cells, pancreatic β-cells are particularly susceptible to ER-stress (89). In this study, the kinetics of one branch of the UPR signalling pathway were characterized in response to pharmacological induction of ER stress. The PERK-dependent ER stress cascade, which controls translational attenuation and regulates the pro-apoptotic transcription factor CHOP, has been proposed to increase apoptosis when chronically sustained, in contrast to IRE1, which has recently been shown to increase proliferation (79). Chronic ER Ca^{2+} depletion, such as that caused by the SERCA inhibitor thapsigargin, caused CHOP induction and apoptosis in MIN6 cells within 24 hours of treatment (81). ER Ca^{2+} release via RyR or IP_3R further participated in this thapsigargin-induced death (81). Previous work has indicated that the ER transmembrane protein PERK is required to initiate Ca^{2+}-dependent ER stress signals (78). The results of the current study indicate that ER Ca^{2+} depletion indeed activates PERK in a rapid manner, and causes eventual apoptosis involving both caspases 7 and 9. This suggests the kinetics of luminal Ca^{2+} depletion can dictate the degree of ER stress, in a PERK-dependent manner.

Palmitate and β-cell ER stress

Previous studies have documented an effect of palmitate on ER-stress in β-cells (20, 68, 70, 74), and these findings are confirmed here in the context of altered Ca^{2+} homeostasis. ER Ca^{2+} levels are critical in the ER stress response (160), and a recent report demonstrated that palmitate-induced CHOP induction was partially mediated by extracellular Ca^{2+} influx (20). Further, a component of the palmitate-induced β-cell death was shown to be due to the rapid and Ca^{2+}-dependent degradation of CPE (61). The present study adds direct ER Ca^{2+}

depletion to the many insults caused by palmitate. The extent of this ER Ca^{2+} release was less than half of that caused by the ER stress-inducer thapsigargin, in the subset of cells that exhibited the palmitate-induced ER Ca^{2+} response. However, since high luminal Ca^{2+} must be maintained for proper protein folding in the ER, the palmitate-induced depletion could be expected to exacerbate ER stress, especially since ER Ca^{2+} levels are important in pro-insulin processing and transport (52). Our study demonstrated rapid PERK phosphorylation after 5 minutes, indicating an immediate response to the palmitate-induced Ca^{2+} release, similar to that observed with thapsigargin. In parallel, another study observed cytokine-induced SERCA down-regulation that resulted in a decrease in ER Ca^{2+} levels and subsequent ER stress induction (18). The observation that chronic palmitate treatment decreased basal ER Ca^{2+} levels is consistent with a recent report (26) and may provide an additional link between ER Ca^{2+} deregulation and cell survival. IRE1 activation has been implicated in palmitate lipotoxicity (26), but we found that blocking ER Ca^{2+} release pharmacologically did not ameliorate this pathway of ER stress, which serves to up-regulate ER chaperone proteins. Whether this arm of the ER stress pathway contributes to β-cell lipotoxicity is unclear, given a recent report that indicated an increase in the ER chaperone protein GPR78 did not inhibit palmitate-induced apoptosis (75). Together, the present study adds another layer to the palmitate-ER stress model, and perhaps establishes the link between ER Ca^{2+} depletion and the onset of ER stress signals by rapid PERK phosphorylation.

Palmitate and lipotoxicity: possible mechanisms

It is clear that a modest Ca^{2+} depletion alone cannot account for β-cell ER stress and cell death. Indeed, chronic palmitate treatment has many deleterious effects on β-cell function

(23, 68, 74, 77, 110) and altered Ca^{2+} homeostasis is an important part of the lipotoxic pathway, but is not sufficient to cause death on its own. For example, blocking extracellular Ca^{2+} influx protects rat islets and cultured cells from palmitate-induced cell death (20, 62), but blocking IP_3R alone did not exert a protective effect (20). Exogenous palmitate may also lead to an accumulation of LC-CoA's, lipid intermediates that can be cytotoxic when in excess via different mechanisms not involving Ca^{2+} signals (28, 107, 131). Further, our study has demonstrated that oleate stimulation creates similar ER Ca^{2+} responses to those of palmitate, and others have shown that this unsaturated fatty acid is indeed less toxic than palmitate (31, 38, 68, 86). Together, these findings indicate that palmitate has multiple deleterious effects on pancreatic β-cells. Results from this study suggest a model whereby chronic palmitate-induced perturbation of ER Ca^{2+} homeostasis contributes to defects in pro-insulin processing (62) and eventually ER stress and apoptosis (**Fig. 18**). This model can help explain β-cell apoptosis in the context of hyperlipidemia, where peripheral insulin resistance or hyperglycemia put an increased demand on insulin biosynthesis. It is worth noting that all our palmitate experiments were done under low glucose conditions, indicating that the lipotoxic effects of palmitate (PERK phosphorylation, ER Ca^{2+} alterations) can occur in low glucose *in vitro*.

Palmitate and insulin secretion

Fatty acids can acutely stimulate insulin secretion in several model systems (98). However, in contrast to previous reports in rodent islets and cultured mouse β-cells (2, 28, 152), palmitate was not a robust insulin secretagogue in MIN6 cells (53). Similarly, palmitate treatment stimulated only a modest acute insulin response in perifused human islets, regardless of whether they were examined in high or low glucose (61). Thus, it is

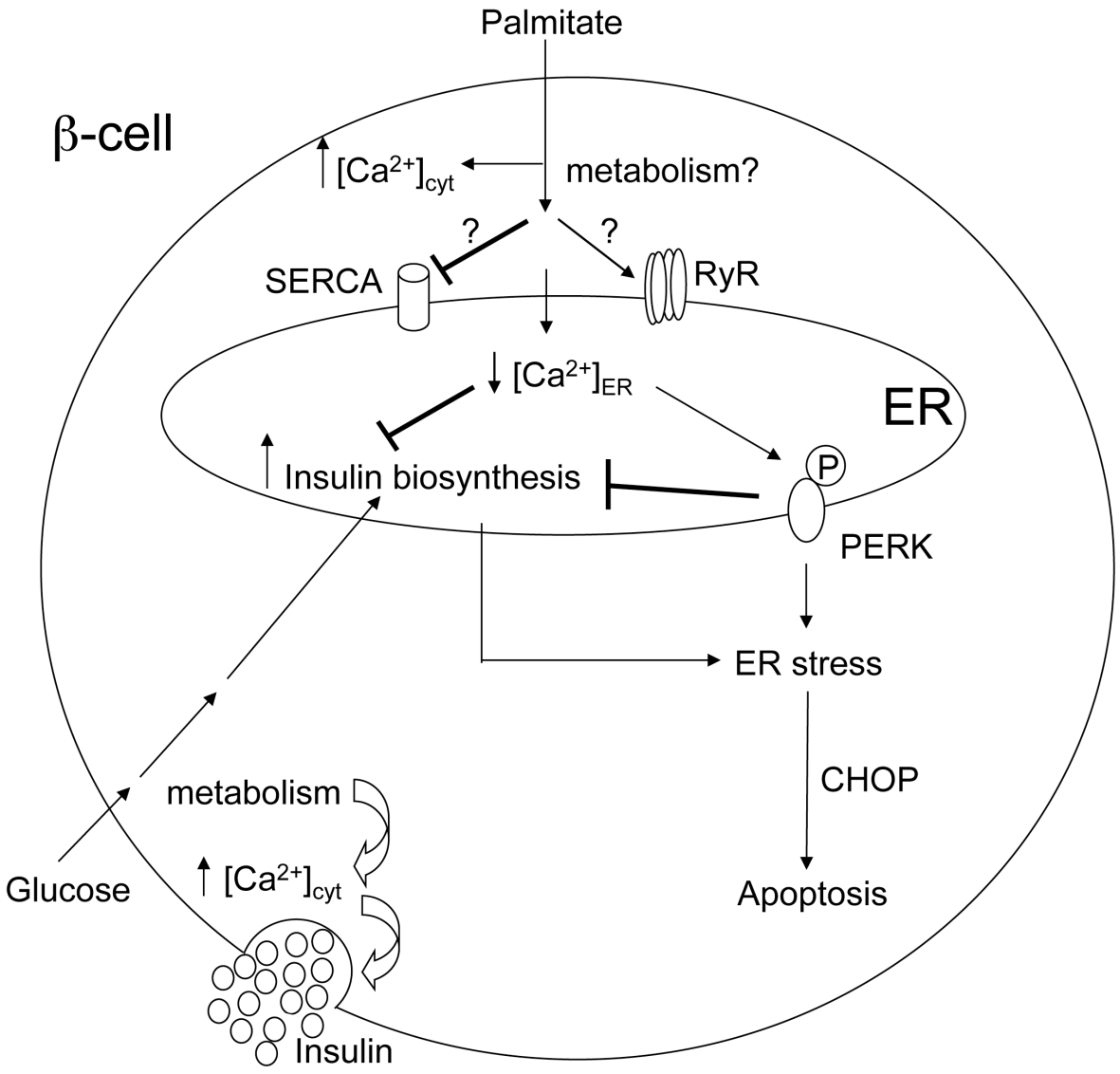

Figure 18. Schematic summarizing palmitate's possible effects on β-cell Ca^{2+} homeostasis and ER stress. $[Ca^{2+}]_{cyt}$ refers to cytosolic Ca^{2+} levels while $[Ca^{2+}]_{ER}$ refers to ER Ca^{2+} levels. Many cellular organelles and other molecules have been left out for clarity.

difficult to confirm studies demonstrating either a palmitate-induced decrease in insulin content or a robust glucose-dependent increase in insulin secretion (107, 153). Together, these data imply that the Ca^{2+} signals generated by palmitate are only weakly coupled to the insulin secretory apparatus in human β-cells and MIN6 cells (53). Perhaps human islets are more similar to MIN6 cells than to mouse islets in this regard. Whether or not this is due to

the spatial location of palmitate-induced Ca^{2+} signals, in that they may not occur near insulin granule exocytotic machinery, remains to be established.

Conclusions and future directions

In conclusion, this project has examined the effects of palmitate on Ca^{2+} signalling in MIN6 cells, using a combination of conventional and new live-cell imaging approaches. Importantly, Ca^{2+} release from the β-cell ER in response to palmitate was directly measured using genetically encoded organelle-targeted probes. The kinetics of PERK activation in response to rapid ER Ca^{2+} depletion were characterized, indicating that fluctuations in ER Ca^{2+} levels can have immediate effects on the cellular ER stress response. In parallel, we found the rapid depletion of ER Ca^{2+} caused by palmitate also stimulated a rapid PERK response, and chronic palmitate treatment affected the basal level of ER Ca^{2+}. This indicates that ER Ca^{2+} levels may contribute to palmitate-induced ER-stress in β-cells. Taken together, these data help define the mechanisms linking hyperlipidemia and β-cell ER stress and eventual failure in type 2 diabetes.

The mechanisms behind palmitate's mobilization of ER Ca^{2+} stores remain to be established, as well as the function of the Ca^{2+} signals themselves. It is clear that disrupted Ca^{2+} homeostasis is not ideal for cell function, and thus it would be worthwhile to further investigate this pathway to perhaps find novel targets for treating type 2 diabetes, as well as other diseases where altered Ca^{2+} signalling is adversely affecting cell survival.

References

1. Aarsland A, and Wolfe RR. Hepatic secretion of VLDL fatty acids during stimulated lipogenesis in men. *J Lipid Res* 39: 1280-1286, 1998.

2. Alcazar O, Qiu-yue Z, Gine E, and Tamarit-Rodriguez J. Stimulation of islet protein kinase C translocation by palmitate requires metabolism of the fatty acid. *Diabetes* 46: 1153-1158, 1997.

3. Alquier T, and Poitout V. GPR40: good cop, bad cop? *Diabetes* 58: 1035-1036, 2009.

4. Alvarez J, and Montero M. Measuring [Ca2+] in the endoplasmic reticulum with aequorin. *Cell Calcium* 32: 251-260, 2002.

5. Ashcroft FM, Harrison DE, and Ashcroft SJ. Glucose induces closure of single potassium channels in isolated rat pancreatic beta-cells. *Nature* 312: 446-448, 1984.

6. Ashworth R, and Brennan C. Use of transgenic zebrafish reporter lines to study calcium signalling in development. *Brief Funct Genomic Proteomic* 4: 186-193, 2005.

7. Bachar E, Ariav Y, Ketzinel-Gilad M, Cerasi E, Kaiser N, and Leibowitz G. Glucose amplifies fatty acid-induced endoplasmic reticulum stress in pancreatic beta-cells via activation of mTORC1. *PLoS ONE* 4: e4954, 2009.

8. Barrett TG, and Bundey SE. Wolfram (DIDMOAD) syndrome. *J Med Genet* 34: 838-841, 1997.

9. Belfort R, Mandarino L, Kashyap S, Wirfel K, Pratipanawatr T, Berria R, Defronzo RA, and Cusi K. Dose-response effect of elevated plasma free fatty acid on insulin signaling. *Diabetes* 54: 1640-1648, 2005.

10. Berridge MJ, Bootman MD, and Roderick HL. Calcium signalling: dynamics, homeostasis and remodelling. *Nat Rev Mol Cell Biol* 4: 517-529, 2003.

11. Berridge MJ, Lipp P, and Bootman MD. The versatility and universality of calcium signalling. *Nat Rev Mol Cell Biol* 1: 11-21, 2000.

12. Boden G. Role of fatty acids in the pathogenesis of insulin resistance and NIDDM. *Diabetes* 46: 3-10, 1997.

13. Boucher A, Lu D, Burgess SC, Telemaque-Potts S, Jensen MV, Mulder H, Wang MY, Unger RH, Sherry AD, and Newgard CB. Biochemical mechanism of lipid-induced impairment of glucose-stimulated insulin secretion and reversal with a malate analogue. *J Biol Chem* 279: 27263-27271, 2004.

14. Brini M, Pinton P, Pozzan T, and Rizzuto R. Targeted recombinant aequorins: tools for monitoring [Ca2+] in the various compartments of a living cell. *Microsc Res Tech* 46: 380-389, 1999.

15. Briscoe CP, Tadayyon M, Andrews JL, Benson WG, Chambers JK, Eilert MM, Ellis C, Elshourbagy NA, Goetz AS, Minnick DT, Murdock PR, Sauls HR, Jr., Shabon U, Spinage LD, Strum JC, Szekeres PG, Tan KB, Way JM, Ignar DM, Wilson S, and Muir AI. The orphan G protein-coupled receptor GPR40 is activated by medium and long chain fatty acids. *J Biol Chem* 278: 11303-11311, 2003.

16. Butler AE, Janson J, Bonner-Weir S, Ritzel R, Rizza RA, and Butler PC. Beta-cell deficit and increased beta-cell apoptosis in humans with type 2 diabetes. *Diabetes* 52: 102-110, 2003.

17. Cabre E, Periago JL, Mingorance MD, Fernandez-Banares F, Abad A, Esteve M, Gil A, Lachica M, Gonzalez-Huix F, and Gassull MA. Factors related to the plasma

fatty acid profile in healthy subjects, with special reference to antioxidant micronutrient status: a multivariate analysis. ***Am J Clin Nutr*** **55: 831-837, 1992.**

18. Cardozo AK, Ortis F, Storling J, Feng YM, Rasschaert J, Tonnesen M, Van Eylen F, Mandrup-Poulsen T, Herchuelz A, and Eizirik DL. Cytokines downregulate the sarcoendoplasmic reticulum pump Ca2+ ATPase 2b and deplete endoplasmic reticulum Ca2+, leading to induction of endoplasmic reticulum stress in pancreatic beta-cells. ***Diabetes*** **54: 452-461, 2005.**

19. Chini EN, and Dousa TP. Palmitoyl-CoA potentiates the Ca2+ release elicited by cyclic ADP-ribose. ***Am J Physiol*** **270: C530-537, 1996.**

20. Choi SE, Kim HE, Shin HC, Jang HJ, Lee KW, Kim Y, Kang SS, Chun J, and Kang Y. Involvement of Ca2+-mediated apoptotic signals in palmitate-induced MIN6N8a beta cell death. ***Mol Cell Endocrinol*** **272: 50-62, 2007.**

21. Cistola DP, and Small DM. Fatty acid distribution in systems modeling the normal and diabetic human circulation. A 13C nuclear magnetic resonance study. ***J Clin Invest*** **87: 1431-1441, 1991.**

22. Clapham DE. Calcium signaling. ***Cell*** **131: 1047-1058, 2007.**

23. Cnop M, Ladriere L, Hekerman P, Ortis F, Cardozo AK, Dogusan Z, Flamez D, Boyce M, Yuan J, and Eizirik DL. Selective inhibition of eukaryotic translation initiation factor 2 alpha dephosphorylation potentiates fatty acid-induced endoplasmic reticulum stress and causes pancreatic beta-cell dysfunction and apoptosis. ***J Biol Chem*** **282: 3989-3997, 2007.**

24. Court JM, Dunlop ME, and Leonard RF. High-frequency oscillation of blood free fatty acid levels in man. ***J Appl Physiol*** **31: 345-347, 1971.**

25. Crespin SR, Greenough WB, 3rd, and Steinberg D. Stimulation of insulin secretion by infusion of free fatty acids. *J Clin Invest* 48: 1934-1943, 1969.

26. Cunha DA, Hekerman P, Ladriere L, Bazarra-Castro A, Ortis F, Wakeham MC, Moore F, Rasschaert J, Cardozo AK, Bellomo E, Overbergh L, Mathieu C, Lupi R, Hai T, Herchuelz A, Marchetti P, Rutter GA, Eizirik DL, and Cnop M. Initiation and execution of lipotoxic ER stress in pancreatic beta-cells. *J Cell Sci* 121: 2308-2318, 2008.

27. De Vos A, Heimberg H, Quartier E, Huypens P, Bouwens L, Pipeleers D, and Schuit F. Human and rat beta cells differ in glucose transporter but not in glucokinase gene expression. *J Clin Invest* 96: 2489-2495, 1995.

28. Deeney JT, Gromada J, Hoy M, Olsen HL, Rhodes CJ, Prentki M, Berggren PO, and Corkey BE. Acute stimulation with long chain acyl-CoA enhances exocytosis in insulin-secreting cells (HIT T-15 and NMRI beta-cells). *J Biol Chem* 275: 9363-9368, 2000.

29. Deeney JT, Tornheim K, Korchak HM, Prentki M, and Corkey BE. Acyl-CoA esters modulate intracellular Ca2+ handling by permeabilized clonal pancreatic beta-cells. *J Biol Chem* 267: 19840-19845, 1992.

30. Delepine M, Nicolino M, Barrett T, Golamaully M, Lathrop GM, and Julier C. EIF2AK3, encoding translation initiation factor 2-alpha kinase 3, is mutated in patients with Wolcott-Rallison syndrome. *Nat Genet* 25: 406-409, 2000.

31. Diakogiannaki E, Dhayal S, Childs CE, Calder PC, Welters HJ, and Morgan NG. Mechanisms involved in the cytotoxic and cytoprotective actions of saturated

versus monounsaturated long-chain fatty acids in pancreatic beta-cells. *J Endocrinol* 194: 283-291, 2007.

32. Diakogiannaki E, Welters HJ, and Morgan NG. Differential regulation of the endoplasmic reticulum stress response in pancreatic beta-cells exposed to long-chain saturated and monounsaturated fatty acids. *J Endocrinol* 197: 553-563, 2008.

33. Dobbins RL, Chester MW, Daniels MB, McGarry JD, and Stein DT. Circulating fatty acids are essential for efficient glucose-stimulated insulin secretion after prolonged fasting in humans. *Diabetes* 47: 1613-1618, 1998.

34. Dobbins RL, Chester MW, Stevenson BE, Daniels MB, Stein DT, and McGarry JD. A fatty acid- dependent step is critically important for both glucose- and non-glucose-stimulated insulin secretion. *J Clin Invest* 101: 2370-2376, 1998.

35. Donath MY, Storling J, Maedler K, and Mandrup-Poulsen T. Inflammatory mediators and islet beta-cell failure: a link between type 1 and type 2 diabetes. *J Mol Med* 81: 455-470, 2003.

36. Dror V, Nguyen V, Walia P, Kalynyak TB, Hill JA, and Johnson JD. Notch signalling suppresses apoptosis in adult human and mouse pancreatic islet cells. *Diabetologia* 50: 2504-2515, 2007.

37. Dryselius S, Grapengiesser E, Hellman B, and Gylfe E. Voltage-dependent entry and generation of slow Ca2+ oscillations in glucose-stimulated pancreatic beta-cells. *Am J Physiol* 276: E512-518, 1999.

38. Eitel K, Staiger H, Brendel MD, Brandhorst D, Bretzel RG, Haring HU, and Kellerer M. Different role of saturated and unsaturated fatty acids in beta-cell apoptosis. *Biochem Biophys Res Commun* 299: 853-856, 2002.

39. Eizirik DL, Cardozo AK, and Cnop M. The Role for Endoplasmic Reticulum Stress in Diabetes Mellitus. *Endocr Rev* 2007.

40. Fex M, Haemmerle G, Wierup N, Dekker-Nitert M, Rehn M, Ristow M, Zechner R, Sundler F, Holm C, Eliasson L, and Mulder H. A beta cell-specific knockout of hormone-sensitive lipase in mice results in hyperglycaemia and disruption of exocytosis. *Diabetologia* 52: 271-280, 2009.

41. Fiala A, and Spall T. In vivo calcium imaging of brain activity in Drosophila by transgenic cameleon expression. *Sci STKE* 2003: PL6, 2003.

42. Fischer H, Koenig U, Eckhart L, and Tschachler E. Human caspase 12 has acquired deleterious mutations. *Biochem Biophys Res Commun* 293: 722-726, 2002.

43. Fitzsimmons TJ, McRoberts JA, Tachiki KH, and Pandol SJ. Acyl-coenzyme A causes Ca2+ release in pancreatic acinar cells. *J Biol Chem* 272: 31435-31440, 1997.

44. Flodgren E, Olde B, Meidute-Abaraviciene S, Winzell MS, Ahren B, and Salehi A. GPR40 is expressed in glucagon producing cells and affects glucagon secretion. *Biochem Biophys Res Commun* 354: 240-245, 2007.

45. Fujiwara K, Maekawa F, Dezaki K, Nakata M, Yashiro T, and Yada T. Oleic acid glucose-independently stimulates glucagon secretion by increasing cytoplasmic Ca2+ via endoplasmic reticulum Ca2+ release and Ca2+ influx in the rat islet alpha-cells. *Endocrinology* 148: 2496-2504, 2007.

46. Fujiwara K, Maekawa F, and Yada T. Oleic acid interacts with GPR40 to induce Ca2+ signaling in rat islet beta-cells: mediation by PLC and L-type Ca2+ channel and link to insulin release. *Am J Physiol Endocrinol Metab* 289: E670-677, 2005.

47. Fulceri R, Knudsen J, Giunti R, Volpe P, Nori A, and Benedetti A. Fatty acyl-CoA-acyl-CoA-binding protein complexes activate the Ca2+ release channel of skeletal muscle sarcoplasmic reticulum. *Biochem J* 325 (Pt 2): 423-428, 1997.

48. Fulceri R, Nori A, Gamberucci A, Volpe P, Giunti R, and Benedetti A. Fatty acyl-CoA esters induce calcium release from terminal cisternae of skeletal muscle. *Cell Calcium* 15: 109-116, 1994.

49. Furstova V, Kopska T, James RF, and Kovar J. Comparison of the effect of individual saturated and unsaturated fatty acids on cell growth and death induction in the human pancreatic beta-cell line NES2Y. *Life Sci* 82: 684-691, 2008.

50. Goh TT, Mason TM, Gupta N, So A, Lam TK, Lam L, Lewis GF, Mari A, and Giacca A. Lipid-induced beta-cell dysfunction in vivo in models of progressive beta-cell failure. *Am J Physiol Endocrinol Metab* 292: E549-560, 2007.

51. Grynkiewicz G, Poenie M, and Tsien RY. A new generation of Ca2+ indicators with greatly improved fluorescence properties. *J Biol Chem* 260: 3440-3450, 1985.

52. Guest PC, Bailyes EM, and Hutton JC. Endoplasmic reticulum Ca2+ is important for the proteolytic processing and intracellular transport of proinsulin in the pancreatic beta-cell. *Biochem J* 323 (Pt 2): 445-450, 1997.

53. Gwiazda KS, Yang TL, Lin Y, and Johnson JD. Effects of palmitate on ER and cytosolic Ca2+ homeostasis in beta-cells. *Am J Physiol Endocrinol Metab* 296: E690-701, 2009.

54. Harding HP, and Ron D. Endoplasmic reticulum stress and the development of diabetes: a review. *Diabetes* 51 Suppl 3: S455-461, 2002.

55. Harding HP, Zeng H, Zhang Y, Jungries R, Chung P, Plesken H, Sabatini DD, and Ron D. Diabetes mellitus and exocrine pancreatic dysfunction in perk-/- mice reveals a role for translational control in secretory cell survival. ***Mol Cell*** **7: 1153-1163, 2001.**

56. Heart E, and Smith PJ. Rhythm of the beta-cell oscillator is not governed by a single regulator: multiple systems contribute to oscillatory behavior. ***Am J Physiol Endocrinol Metab*** **292: E1295-1300, 2007.**

57. Henquin JC. Regulation of insulin secretion: a matter of phase control and amplitude modulation. ***Diabetologia*** **52: 739-751, 2009.**

58. Huang CJ, Lin CY, Haataja L, Gurlo T, Butler AE, Rizza RA, and Butler PC. High expression rates of human islet amyloid polypeptide induce endoplasmic reticulum stress mediated beta-cell apoptosis, a characteristic of humans with type 2 but not type 1 diabetes. ***Diabetes*** **56: 2016-2027, 2007.**

59. Hui H, Dotta F, Di Mario U, and Perfetti R. Role of caspases in the regulation of apoptotic pancreatic islet beta-cells death. ***J Cell Physiol*** **200: 177-200, 2004.**

60. Itoh Y, Kawamata Y, Harada M, Kobayashi M, Fujii R, Fukusumi S, Ogi K, Hosoya M, Tanaka Y, Uejima H, Tanaka H, Maruyama M, Satoh R, Okubo S, Kizawa H, Komatsu H, Matsumura F, Noguchi Y, Shinohara T, Hinuma S, Fujisawa Y, and Fujino M. Free fatty acids regulate insulin secretion from pancreatic beta cells through GPR40. ***Nature*** **422: 173-176, 2003.**

61. Jeffrey KD, Alejandro EU, Luciani DS, Kalynyak TB, Hu X, Li H, Lin Y, Townsend RR, Polonsky KS, and Johnson JD. Carboxypeptidase E mediates palmitate-induced {beta}-cell ER stress and apoptosis. ***Proc Natl Acad Sci U S A*** **2008.**

62. Jeffrey KD, Alejandro EU, Luciani DS, Kalynyak TB, Hu X, Li H, Lin Y, Townsend RR, Polonsky KS, and Johnson JD. Carboxypeptidase E mediates palmitate-induced beta-cell ER stress and apoptosis. ***Proc Natl Acad Sci U S A*** **105: 8452-8457, 2008.**

63. Jensen MV, Joseph JW, Ronnebaum SM, Burgess SC, Sherry AD, and Newgard CB. Metabolic cycling in control of glucose-stimulated insulin secretion. ***Am J Physiol Endocrinol Metab*** **295: E1287-1297, 2008.**

64. Johnson JD, Ahmed NT, Luciani DS, Han Z, Tran H, Fujita J, Misler S, Edlund H, and Polonsky KS. Increased islet apoptosis in Pdx1+/- mice. ***J Clin Invest*** **111: 1147-1160, 2003.**

65. Johnson JD, Han Z, Otani K, Ye H, Zhang Y, Wu H, Horikawa Y, Misler S, Bell GI, and Polonsky KS. RyR2 and calpain-10 delineate a novel apoptosis pathway in pancreatic islets. ***J Biol Chem*** **279: 24794-24802, 2004.**

66. Johnson JD, and Misler S. Nicotinic acid-adenine dinucleotide phosphate-sensitive calcium stores initiate insulin signaling in human beta cells. ***Proc Natl Acad Sci U S A*** **99: 14566-14571, 2002.**

67. Kahn SE, Hull RL, and Utzschneider KM. Mechanisms linking obesity to insulin resistance and type 2 diabetes. ***Nature*** **444: 840-846, 2006.**

68. Karaskov E, Scott C, Zhang L, Teodoro T, Ravazzola M, and Volchuk A. Chronic palmitate but not oleate exposure induces endoplasmic reticulum stress, which may contribute to INS-1 pancreatic beta-cell apoptosis. ***Endocrinology*** **147: 3398-3407, 2006.**

69. Kebede M, Alquier T, Latour MG, Semache M, Tremblay C, and Poitout V. The fatty acid receptor GPR40 plays a role in insulin secretion in vivo after high-fat feeding. *Diabetes* 57: 2432-2437, 2008.

70. Kharroubi I, Ladriere L, Cardozo AK, Dogusan Z, Cnop M, and Eizirik DL. Free fatty acids and cytokines induce pancreatic beta-cell apoptosis by different mechanisms: role of nuclear factor-kappaB and endoplasmic reticulum stress. *Endocrinology* 145: 5087-5096, 2004.

71. Kiekens R, In 't Veld P, Mahler T, Schuit F, Van De Winkel M, and Pipeleers D. Differences in glucose recognition by individual rat pancreatic B cells are associated with intercellular differences in glucose-induced biosynthetic activity. *J Clin Invest* 89: 117-125, 1992.

72. Koshkin V, Dai FF, Robson-Doucette CA, Chan CB, and Wheeler MB. Limited mitochondrial permeabilization is an early manifestation of palmitate-induced lipotoxicity in pancreatic beta-cells. *J Biol Chem* 283: 7936-7948, 2008.

73. Kotarsky K, Nilsson NE, Flodgren E, Owman C, and Olde B. A human cell surface receptor activated by free fatty acids and thiazolidinedione drugs. *Biochem Biophys Res Commun* 301: 406-410, 2003.

74. Lai E, Bikopoulos G, Wheeler MB, Rozakis-Adcock M, and Volchuk A. Differential activation of ER stress and apoptosis in response to chronically elevated free fatty acids in pancreatic {beta}-cells. *Am J Physiol Endocrinol Metab* 294: E540-550, 2008.

75. Lai E, Bikopoulos G, Wheeler MB, Rozakis-Adcock M, and Volchuk A. Differential activation of ER stress and apoptosis in response to chronically elevated

free fatty acids in pancreatic beta-cells. *Am J Physiol Endocrinol Metab* 294: E540-550, 2008.

76. Latour MG, Alquier T, Oseid E, Tremblay C, Jetton TL, Luo J, Lin DC, and Poitout V. GPR40 is necessary but not sufficient for fatty acid stimulation of insulin secretion in vivo. *Diabetes* 56: 1087-1094, 2007.

77. Laybutt DR, Preston AM, Akerfeldt MC, Kench JG, Busch AK, Biankin AV, and Biden TJ. Endoplasmic reticulum stress contributes to beta cell apoptosis in type 2 diabetes. *Diabetologia* 50: 752-763, 2007.

78. Liang SH, Zhang W, McGrath BC, Zhang P, and Cavener DR. PERK (eIF2alpha kinase) is required to activate the stress-activated MAPKs and induce the expression of immediate-early genes upon disruption of ER calcium homoeostasis. *Biochem J* 393: 201-209, 2006.

79. Lin JH, Li H, Zhang Y, Ron D, and Walter P. Divergent effects of PERK and IRE1 signaling on cell viability. *PLoS ONE* 4: e4170, 2009.

80. Luciani DS, Ao P, Hu X, Warnock GL, and Johnson JD. Voltage-gated Ca(2+) influx and insulin secretion in human and mouse beta-cells are impaired by the mitochondrial Na(+)/Ca(2+) exchange inhibitor CGP-37157. *Eur J Pharmacol* 576: 18-25, 2007.

81. Luciani DS, Gwiazda K, Yang TL, Kalynyak TB, Bychkivska Y, Frey MH, Jeffrey KD, Sampaio AV, Underhill TM, and Johnson JD. Roles of IP3R and RyR Ca2+ Channels in Endoplasmic Reticulum Stress and {beta}-Cell Death. *Diabetes* 2008.

82. Luciani DS, Misler S, and Polonsky KS. Ca2+ controls slow NAD(P)H oscillations in glucose-stimulated mouse pancreatic islets. *J Physiol* 572: 379-392, 2006.

83. Lupi R, Dotta F, Marselli L, Del Guerra S, Masini M, Santangelo C, Patane G, Boggi U, Piro S, Anello M, Bergamini E, Mosca F, Di Mario U, Del Prato S, and Marchetti P. Prolonged exposure to free fatty acids has cytostatic and pro-apoptotic effects on human pancreatic islets: evidence that beta-cell death is caspase mediated, partially dependent on ceramide pathway, and Bcl-2 regulated. *Diabetes* 51: 1437-1442, 2002.

84. MacDonald PE, and Rorsman P. The ins and outs of secretion from pancreatic beta-cells: control of single-vesicle exo- and endocytosis. *Physiology (Bethesda)* 22: 113-121, 2007.

85. Maedler K, Oberholzer J, Bucher P, Spinas GA, and Donath MY. Monounsaturated fatty acids prevent the deleterious effects of palmitate and high glucose on human pancreatic beta-cell turnover and function. *Diabetes* 52: 726-733, 2003.

86. Maedler K, Spinas GA, Dyntar D, Moritz W, Kaiser N, and Donath MY. Distinct effects of saturated and monounsaturated fatty acids on beta-cell turnover and function. *Diabetes* 50: 69-76, 2001.

87. Maestre I, Jordan J, Calvo S, Reig JA, Cena V, Soria B, Prentki M, and Roche E. Mitochondrial dysfunction is involved in apoptosis induced by serum withdrawal and fatty acids in the beta-cell line INS-1. *Endocrinology* 144: 335-345, 2003.

88. Mandic A, Hansson J, Linder S, and Shoshan MC. Cisplatin induces endoplasmic reticulum stress and nucleus-independent apoptotic signaling. *J Biol Chem* 278: 9100-9106, 2003.

89. Marchetti P, Bugliani M, Lupi R, Marselli L, Masini M, Boggi U, Filipponi F, Weir GC, Eizirik DL, and Cnop M. The endoplasmic reticulum in pancreatic beta cells of type 2 diabetes patients. *Diabetologia* 50: 2486-2494, 2007.

90. Martinez SC, Tanabe K, Cras-Meneur C, Abumrad NA, Bernal-Mizrachi E, and Permutt MA. Inhibition of Foxo1 protects pancreatic islet beta-cells against fatty acid and endoplasmic reticulum stress-induced apoptosis. *Diabetes* 57: 846-859, 2008.

91. Matsuzaka T, Shimano H, Yahagi N, Kato T, Atsumi A, Yamamoto T, Inoue N, Ishikawa M, Okada S, Ishigaki N, Iwasaki H, Iwasaki Y, Karasawa T, Kumadaki S, Matsui T, Sekiya M, Ohashi K, Hasty AH, Nakagawa Y, Takahashi A, Suzuki H, Yatoh S, Sone H, Toyoshima H, Osuga J, and Yamada N. Crucial role of a long-chain fatty acid elongase, Elovl6, in obesity-induced insulin resistance. *Nat Med* 13: 1193-1202, 2007.

92. Matveyenko AV, Gurlo T, Daval M, Butler AE, and Butler PC. Successful versus failed adaptation to high-fat diet-induced insulin resistance: the role of IAPP-induced beta-cell endoplasmic reticulum stress. *Diabetes* 58: 906-916, 2009.

93. McCombs JE, and Palmer AE. Measuring calcium dynamics in living cells with genetically encodable calcium indicators. *Methods* 46: 152-159, 2008.

94. Meex SJ, van Greevenbroek MM, Ayoubi TA, Vlietinck R, van Vliet-Ostaptchouk JV, Hofker MH, Vermeulen VM, Schalkwijk CG, Feskens EJ, Boer JM, Stehouwer CD, van der Kallen CJ, and de Bruin TW. Activating transcription factor 6 polymorphisms and haplotypes are associated with impaired glucose homeostasis and type 2 diabetes in Dutch Caucasians. *J Clin Endocrinol Metab* 92: 2720-2725, 2007.

95. Miyazaki J, Araki K, Yamato E, Ikegami H, Asano T, Shibasaki Y, Oka Y, and Yamamura K. Establishment of a pancreatic beta cell line that retains glucose-inducible insulin secretion: special reference to expression of glucose transporter isoforms. *Endocrinology* 127: 126-132, 1990.

96. Nagasumi K, Esaki R, Iwachidow K, Yasuhara Y, Ogi K, Tanaka H, Nakata M, Yano T, Shimakawa K, Taketomi S, Takeuchi K, Odaka H, and Kaisho Y. Overexpression of GPR40 in pancreatic beta-cells augments glucose-stimulated insulin secretion and improves glucose tolerance in normal and diabetic mice. *Diabetes* 58: 1067-1076, 2009.

97. Nolan CJ, Leahy JL, Delghingaro-Augusto V, Moibi J, Soni K, Peyot ML, Fortier M, Guay C, Lamontagne J, Barbeau A, Przybytkowski E, Joly E, Masiello P, Wang S, Mitchell GA, and Prentki M. Beta cell compensation for insulin resistance in Zucker fatty rats: increased lipolysis and fatty acid signalling. *Diabetologia* 49: 2120-2130, 2006.

98. Nolan CJ, Madiraju MS, Delghingaro-Augusto V, Peyot ML, and Prentki M. Fatty acid signaling in the beta-cell and insulin secretion. *Diabetes* 55 Suppl 2: S16-23, 2006.

99. Noushmehr H, D'Amico E, Farilla L, Hui H, Wawrowsky KA, Mlynarski W, Doria A, Abumrad NA, and Perfetti R. Fatty acid translocase (FAT/CD36) is localized on insulin-containing granules in human pancreatic beta-cells and mediates fatty acid effects on insulin secretion. *Diabetes* 54: 472-481, 2005.

100. Nunemaker CS, Bertram R, Sherman A, Tsaneva-Atanasova K, Daniel CR, and Satin LS. Glucose modulates [Ca2+]i oscillations in pancreatic islets via ionic and glycolytic mechanisms. *Biophys J* 91: 2082-2096, 2006.

101. Olofsson CS, Salehi A, Holm C, and Rorsman P. Palmitate increases L-type Ca2+ currents and the size of the readily releasable granule pool in mouse pancreatic beta-cells. *J Physiol* 557: 935-948, 2004.

102. Oprescu AI, Bikopoulos G, Naassan A, Allister EM, Tang C, Park E, Uchino H, Lewis GF, Fantus IG, Rozakis-Adcock M, Wheeler MB, and Giacca A. Free fatty acid-induced reduction in glucose-stimulated insulin secretion: evidence for a role of oxidative stress in vitro and in vivo. *Diabetes* 56: 2927-2937, 2007.

103. Oyadomari S, Koizumi A, Takeda K, Gotoh T, Akira S, Araki E, and Mori M. Targeted disruption of the Chop gene delays endoplasmic reticulum stress-mediated diabetes. *J Clin Invest* 109: 525-532, 2002.

104. Palmer AE. Expanding the repertoire of fluorescent calcium sensors. *ACS Chem Biol* 4: 157-159, 2009.

105. Palmer AE, Jin C, Reed JC, and Tsien RY. Bcl-2-mediated alterations in endoplasmic reticulum Ca2+ analyzed with an improved genetically encoded fluorescent sensor. *Proc Natl Acad Sci U S A* 101: 17404-17409, 2004.

106. Palmer AE, and Tsien RY. Measuring calcium signaling using genetically targetable fluorescent indicators. *Nat Protoc* 1: 1057-1065, 2006.

107. Parker SM, Moore PC, Johnson LM, and Poitout V. Palmitate potentiation of glucose-induced insulin release: a study using 2-bromopalmitate. *Metabolism* 52: 1367-1371, 2003.

108. Paumen MB, Ishida Y, Muramatsu M, Yamamoto M, and Honjo T. Inhibition of carnitine palmitoyltransferase I augments sphingolipid synthesis and palmitate-induced apoptosis. *J Biol Chem* 272: 3324-3329, 1997.

109. Peyot ML, Guay C, Latour MG, Lamontagne J, Lussier R, Pineda M, Ruderman NB, Haemmerle G, Zechner R, Joly E, Madiraju SR, Poitout V, and Prentki M. Adipose triglyceride lipase is implicated in fuel and non-fuel stimulated insulin secretion. *J Biol Chem* 2009.

110. Piro S, Anello M, Di Pietro C, Lizzio MN, Patane G, Rabuazzo AM, Vigneri R, Purrello M, and Purrello F. Chronic exposure to free fatty acids or high glucose induces apoptosis in rat pancreatic islets: possible role of oxidative stress. *Metabolism* 51: 1340-1347, 2002.

111. Poitout V. Glucolipotoxicity of the pancreatic beta-cell: myth or reality? *Biochem Soc Trans* 36: 901-904, 2008.

112. Poitout V, and Robertson RP. Glucolipotoxicity: fuel excess and beta-cell dysfunction. *Endocr Rev* 29: 351-366, 2008.

113. Prentki M, Joly E, El-Assaad W, and Roduit R. Malonyl-CoA signaling, lipid partitioning, and glucolipotoxicity: role in beta-cell adaptation and failure in the etiology of diabetes. *Diabetes* 51 Suppl 3: S405-413, 2002.

114. Prentki M, and Nolan CJ. Islet beta cell failure in type 2 diabetes. *J Clin Invest* 116: 1802-1812, 2006.

115. Rahier J, Goebbels RM, and Henquin JC. Cellular composition of the human diabetic pancreas. *Diabetologia* 24: 366-371, 1983.

116. Rebuffe-Scrive M, Anderson B, Olbe L, and Bjorntorp P. Metabolism of adipose tissue in intraabdominal depots in severely obese men and women. *Metabolism* 39: 1021-1025, 1990.

117. Reitsma WD. The relationship between serum free fatty acids and blood sugar in non-obese and obese diabetics. *Acta Med Scand* 182: 353-361, 1967.

118. Remizov O, Jakubov R, Dufer M, Krippeit Drews P, Drews G, Waring M, Brabant G, Wienbergen A, Rustenbeck I, and Schofl C. Palmitate-induced Ca2+-signaling in pancreatic beta-cells. *Mol Cell Endocrinol* 212: 1-9, 2003.

119. Resh MD. Use of analogs and inhibitors to study the functional significance of protein palmitoylation. *Methods* 40: 191-197, 2006.

120. Richieri GV, Anel A, and Kleinfeld AM. Interactions of long-chain fatty acids and albumin: determination of free fatty acid levels using the fluorescent probe ADIFAB. *Biochemistry* 32: 7574-7580, 1993.

121. Richieri GV, and Kleinfeld AM. Unbound free fatty acid levels in human serum. *J Lipid Res* 36: 229-240, 1995.

122. Rizzuto R, and Pozzan T. Microdomains of intracellular Ca2+: molecular determinants and functional consequences. *Physiol Rev* 86: 369-408, 2006.

123. Roduit R, Nolan C, Alarcon C, Moore P, Barbeau A, Delghingaro-Augusto V, Przybykowski E, Morin J, Masse F, Massie B, Ruderman N, Rhodes C, Poitout V, and Prentki M. A role for the malonyl-CoA/long-chain acyl-CoA pathway of lipid signaling in the regulation of insulin secretion in response to both fuel and nonfuel stimuli. *Diabetes* 53: 1007-1019, 2004.

124. Roglic G, Unwin N, Bennett PH, Mathers C, Tuomilehto J, Nag S, Connolly V, and King H. The burden of mortality attributable to diabetes: realistic estimates for the year 2000. *Diabetes Care* 28: 2130-2135, 2005.

125. Sako Y, and Grill VE. A 48-hour lipid infusion in the rat time-dependently inhibits glucose-induced insulin secretion and B cell oxidation through a process likely coupled to fatty acid oxidation. *Endocrinology* 127: 1580-1589, 1990.

126. Sakuraba H, Mizukami H, Yagihashi N, Wada R, Hanyu C, and Yagihashi S. Reduced beta-cell mass and expression of oxidative stress-related DNA damage in the islet of Japanese Type II diabetic patients. *Diabetologia* 45: 85-96, 2002.

127. Salehi A, Flodgren E, Nilsson NE, Jimenez-Feltstrom J, Miyazaki J, Owman C, and Olde B. Free fatty acid receptor 1 (FFA(1)R/GPR40) and its involvement in fatty-acid-stimulated insulin secretion. *Cell Tissue Res* 322: 207-215, 2005.

128. Scheuner D, and Kaufman RJ. The unfolded protein response: a pathway that links insulin demand with beta-cell failure and diabetes. *Endocr Rev* 29: 317-333, 2008.

129. Schnell S, Schaefer M, and Schofl C. Free fatty acids increase cytosolic free calcium and stimulate insulin secretion from beta-cells through activation of GPR40. *Mol Cell Endocrinol* 263: 173-180, 2007.

130. Schroder M, and Kaufman RJ. The mammalian unfolded protein response. *Annu Rev Biochem* 74: 739-789, 2005.

131. Schulze D, Rapedius M, Krauter T, and Baukrowitz T. Long-chain acyl-CoA esters and phosphatidylinositol phosphates modulate ATP inhibition of KATP channels by the same mechanism. *J Physiol* 552: 357-367, 2003.

132. Shimabukuro M, Zhou YT, Levi M, and Unger RH. Fatty acid-induced beta cell apoptosis: a link between obesity and diabetes. *Proc Natl Acad Sci U S A* 95: 2498-2502, 1998.

133. Song B, Scheuner D, Ron D, Pennathur S, and Kaufman RJ. Chop deletion reduces oxidative stress, improves beta cell function, and promotes cell survival in multiple mouse models of diabetes. *J Clin Invest* 118: 3378-3389, 2008.

134. Spector AA. Fatty acid binding to plasma albumin. *J Lipid Res* 16: 165-179, 1975.

135. Spector AA, and Hoak JC. Letter: Fatty acids, platelets, and microcirculatory obstruction. *Science* 190: 490-492, 1975.

136. Steneberg P, Rubins N, Bartoov-Shifman R, Walker MD, and Edlund H. The FFA receptor GPR40 links hyperinsulinemia, hepatic steatosis, and impaired glucose homeostasis in mouse. *Cell Metab* 1: 245-258, 2005.

137. Stoy J, Edghill EL, Flanagan SE, Ye H, Paz VP, Pluzhnikov A, Below JE, Hayes MG, Cox NJ, Lipkind GM, Lipton RB, Greeley SA, Patch AM, Ellard S, Steiner DF, Hattersley AT, Philipson LH, and Bell GI. Insulin gene mutations as a cause of permanent neonatal diabetes. *Proc Natl Acad Sci U S A* 104: 15040-15044, 2007.

138. Strawford A, Antelo F, Christiansen M, and Hellerstein MK. Adipose tissue triglyceride turnover, de novo lipogenesis, and cell proliferation in humans measured with 2H2O. *Am J Physiol Endocrinol Metab* 286: E577-588, 2004.

139. Stubbs CD, and Smith AD. Essential fatty acids in membrane: physical properties and function. *Biochem Soc Trans* 18: 779-781, 1990.

140. Szegezdi E, Fitzgerald U, and Samali A. Caspase-12 and ER-stress-mediated apoptosis: the story so far. *Ann N Y Acad Sci* 1010: 186-194, 2003.

141. Tan CP, Feng Y, Zhou YP, Eiermann GJ, Petrov A, Zhou C, Lin S, Salituro G, Meinke P, Mosley R, Akiyama TE, Einstein M, Kumar S, Berger JP, Mills SG, Thornberry NA, Yang L, and Howard AD. Selective small-molecule agonists of G protein-coupled receptor 40 promote glucose-dependent insulin secretion and reduce blood glucose in mice. *Diabetes* 57: 2211-2219, 2008.

142. Tengholm A, and Gylfe E. Oscillatory control of insulin secretion. *Mol Cell Endocrinol* 297: 58-72, 2009.

143. Thameem F, Farook VS, Bogardus C, and Prochazka M. Association of amino acid variants in the activating transcription factor 6 gene (ATF6) on 1q21-q23 with type 2 diabetes in Pima Indians. *Diabetes* 55: 839-842, 2006.

144. Thomas D, Tovey SC, Collins TJ, Bootman MD, Berridge MJ, and Lipp P. A comparison of fluorescent Ca2+ indicator properties and their use in measuring elementary and global Ca2+ signals. *Cell Calcium* 28: 213-223, 2000.

145. Tian Y, Corkey RF, Yaney GC, Goforth PB, Satin LS, and Moitoso de Vargas L. Differential modulation of L-type calcium channel subunits by oleate. *Am J Physiol Endocrinol Metab* 294: E1178-1186, 2008.

146. Unger RH, and Orci L. Lipoapoptosis: its mechanism and its diseases. *Biochim Biophys Acta* 1585: 202-212, 2002.

147. Urano F, Wang X, Bertolotti A, Zhang Y, Chung P, Harding HP, and Ron D. Coupling of stress in the ER to activation of JNK protein kinases by transmembrane protein kinase IRE1. *Science* 287: 664-666, 2000.

148. Van Schravendijk CF, Kiekens R, Heylen L, and Pipeleers DG. Amino-acid responsiveness in beta cell subpopulations with different sensitivity to glucose. *Biochem Biophys Res Commun* 204: 490-497, 1994.

149. Van Schravendijk CF, Kiekens R, and Pipeleers DG. Pancreatic beta cell heterogeneity in glucose-induced insulin secretion. *J Biol Chem* 267: 21344-21348, 1992.

150. Wang H, Kouri G, and Wollheim CB. ER stress and SREBP-1 activation are implicated in beta-cell glucolipotoxicity. *J Cell Sci* 118: 3905-3915, 2005.

151. Wang J, Baimbridge KG, and Brown JC. Glucose- and acetylcholine-induced increase in intracellular free Ca2+ in subpopulations of individual rat pancreatic beta-cells. *Endocrinology* 131: 146-152, 1992.

152. Warnotte C, Gilon P, Nenquin M, and Henquin JC. Mechanisms of the stimulation of insulin release by saturated fatty acids. A study of palmitate effects in mouse beta-cells. *Diabetes* 43: 703-711, 1994.

153. Warnotte C, Nenquin M, and Henquin JC. Unbound rather than total concentration and saturation rather than unsaturation determine the potency of fatty acids on insulin secretion. *Mol Cell Endocrinol* 153: 147-153, 1999.

154. Westermark PO, and Lansner A. A model of phosphofructokinase and glycolytic oscillations in the pancreatic beta-cell. *Biophys J* 85: 126-139, 2003.

155. WHO. Diabetes [fact sheet] http://www.who.int/mediacentre/factsheets/fs312/en/.

156. Wild S, Roglic G, Green A, Sicree R, and King H. Global prevalence of diabetes: estimates for the year 2000 and projections for 2030. *Diabetes Care* 27: 1047-1053, 2004.

157. Wiser O, Trus M, Hernandez A, Renstrom E, Barg S, Rorsman P, and Atlas D. The voltage sensitive Lc-type Ca2+ channel is functionally coupled to the exocytotic machinery. *Proc Natl Acad Sci U S A* 96: 248-253, 1999.

158. Xiao C, Giacca A, Carpentier A, and Lewis GF. Differential effects of monounsaturated, polyunsaturated and saturated fat ingestion on glucose-stimulated insulin secretion, sensitivity and clearance in overweight and obese, non-diabetic humans. *Diabetologia* 49: 1371-1379, 2006.

159. Xie Q, Khaoustov VI, Chung CC, Sohn J, Krishnan B, Lewis DE, and Yoffe B. Effect of tauroursodeoxycholic acid on endoplasmic reticulum stress-induced caspase-12 activation. *Hepatology* 36: 592-601, 2002.

160. Xu C, Bailly-Maitre B, and Reed JC. Endoplasmic reticulum stress: cell life and death decisions. *J Clin Invest* 115: 2656-2664, 2005.

161. Yoon KH, Ko SH, Cho JH, Lee JM, Ahn YB, Song KH, Yoo SJ, Kang MI, Cha BY, Lee KW, Son HY, Kang SK, Kim HS, Lee IK, and Bonner-Weir S. Selective beta-cell loss and alpha-cell expansion in patients with type 2 diabetes mellitus in Korea. *J Clin Endocrinol Metab* 88: 2300-2308, 2003.

162. Zhou YP, and Grill V. Long term exposure to fatty acids and ketones inhibits B-cell functions in human pancreatic islets of Langerhans. *J Clin Endocrinol Metab* 80: 1584-1590, 1995.

163. Zhou YP, and Grill VE. Long-term exposure of rat pancreatic islets to fatty acids inhibits glucose-induced insulin secretion and biosynthesis through a glucose fatty acid cycle. *J Clin Invest* 93: 870-876, 1994.